Spring 2017

Real-time prediction of stream water temperature for Iowa

Yibing Su
University of Iowa

REAL-TIME PREDICTION OF STREAM WATER TEMPERATURE FOR IOWA

by
Yibing Su

A thesis submitted in partial fulfillment
of the requirements for the Master of
Science degree in Civil and Environmental Engineering
in the Graduate College of
The University of Iowa

May 2017

Thesis Supervisor: Professor Witold F. Krajewski

Graduate College
The University of Iowa
Iowa City, Iowa

CERTIFICATE OF APPROVAL

_____

MASTER'S THESIS

_____

This is to certify that the Master's thesis of

Yibing Su

has been approved by the Examining Committee
for the thesis requirement for the Master of Science
degree in Civil and Environmental Engineering at the May 2017 graduation.

Thesis Committee: _____
Witold F. Krajewski, Thesis Supervisor

_____
A. Allen Bradley, Jr.

_____
Larry J. Weber

ACKNOWLEDGMENTS

First and foremost, I would like to thank my advisor Witold Krajewski. For the past five years as I set out on the path of engineering and academics, Professor Krajewski, you have been my invaluable source of guidance and support. You have not only steered me to the direction that I have chosen today, but have also shown me perspective and vision to carry me forward. Dr. Allen Bradley, your knowledge, advice, and the perfect sense of structure and organization in everything you do, has made me grow increasingly fond of the engineering profession. Dr. Larry Weber, your insight has greatly contributed to the success of this work.

I would also like to thank my friends at IIHR - Hydroscience & Engineering, the University of Iowa, and back home in China. Your friendship has been my source of motivation. To Sam Debionne, I would especially like to thank you for sharing your knowledge and guiding me.

Finally, I would like to acknowledge my mother, who has always provided me with endless love and encouragement. If not for your faith, wisdom, and vision, I would never have come so far in my life. “Like arrows in the hand of a warrior are the children of one’s youth.” -- Psalm 127:4

I give my praise to the Lord for providing me the ability to seek order in the seemingly chaotic but beautiful world

ABSTRACT

In the agricultural state of Iowa, water quality research is of great importance for monitoring and managing the health of aquatic systems. Among many water quality parameters, water temperature is a critical variable that governs the rates of chemical and biological processes which affect river health. The main objective of this thesis is to develop a real-time high resolution predictive stream temperature model for the entire state of Iowa. A statistical model based solely on the water-air temperature relationship was developed using logistic regression approach. With hourly High Resolution Rapid Refresh (HRRR) air temperature estimations, the implemented stream temperature model produces current state-wide estimations. The results are updated hourly in real-time and presented on a web-based visualization platform: the Iowa Water Quality Information System, Beta version (IWQIS Beta). Streams of 4^{th} order and up are color-coded according to the estimated temperatures. Hourly forecasts for lead time of up to 18 hours are also available.

A model was developed separately for spring (March to May), summer (June to August), and autumn (September to November) seasons. 2016 model estimation results generate less than 3 °C average RMSE for the three seasons, with a summer season RMSE of below 2 °C. The model is transferrable to basins of different catchment sizes within the state of Iowa and requires hourly air temperature as the only input variable. The product will assist Iowa water quality research and provide information to support public management decisions.

PUBLIC ABSTRACT

In the agricultural state of Iowa, water quality research is of great importance for monitoring and managing aquatic systems health. Among many water quality parameters, water temperature is a critical variable that governs the rates of chemical and biological processes which affect river health. A statistical model was developed to produce real-time high resolution predictive stream temperature for the entire state of Iowa. The implemented model generates current-hour stream temperature estimations state-wide. Forecasts for 18 hours in advance are also available. The hourly estimation results are updated in real-time and presented on a web-based visualization platform: the Iowa Water Quality Information System, Beta version (IWQIS Beta). This product will assist Iowa water quality research and provide information to support public management decisions.

TABLE OF CONTENTS

LIST OF TABLES

LIST OF FIGURES

CHAPTER 1 INTRODUCTION

1.1 Background & Motivation

As one of the controlling influencers of aquatic habitat, water temperature has great economic and ecological significance. Water temperature strongly relates to the biological and chemical processes in streams, as well as fish habitat distribution. Due to the relationship between in-stream microbial activities and stream temperature, nutrient growth/removal models often include stream temperature as a predictor (Crumpton, Stenback, Miller, & Helmers, 2006). The United States Environmental Protection Agency (U.S. EPA) has been establishing Regional Monitoring Networks (RMNs) to document current conditions and detect long-term changes in biological, thermal, hydrologic, physical habitat and water chemistry for freshwater wadeable streams (EPA, 2016). Among the many metrics being documented, water temperature is an important parameter that indicates the overall health of the stream ecosystem. Studies of anthropogenic perturbations, such as power plant cooling and global warming, and their impact on stream temperature, have also been attracting increased attention.

In the state of Iowa, rural farms compose about 92.6% of the total land (Iowa State University Extension and Outreach, 2017). The high agricultural land rate introduces significant water pollution problems in Iowa. Hence water quality in the rivers and streams of Iowa has been one of the main focus areas studied at IIHR-Hydroscience & Engineering (IIHR) by the Iowa Nutrient Research Center (INRC) group. Various water quality parameters and their effects on stream health are being monitored and modeled. Additionally, the trout survival rate in north-eastern Iowa streams is also of

interest. Therefore, a need for dense spatially distributed stream temperature data arises. Hourly temporal resolution is desired to capture the stream temperature diurnal cycle behavior. Hence this thesis project aims to develop, evaluate, and implement a state-wide stream temperature model that is able to generate real-time estimation with fine spatial and temporal resolutions.

The four main categories of factors influencing stream water temperature are atmospheric conditions, topography, discharge, and streambed, as demonstrated in Figure 1.1. In order to predict stream water temperature, we have at hand a thermodynamics problem. A full-scale deterministic model that applies an energy balance approach takes into consideration various parameters including solar radiation, sensible heat flux, latent heat flux, evaporative flux, channel velocity, channel depth, relative humidity, wind speed, cloud cover, riparian vegetation cover, groundwater seepage, discharge, and artificial heat inputs. Such a model estimates stream water temperature by solving a partial differential equation with respect to space and time, as shown in Equation (1),

$$\frac{\partial T}{\partial t} = -U\frac{\partial T}{\partial x} + D_L\frac{\partial^2 T}{\partial x^2} + \frac{S}{\rho C_p d} \tag{1}$$

where U is mean channel velocity, D_L is dispersion factor, ρ is the density of water, C_p is the specific heat of water, d is mean depth of channel, and S is source and sink of heat fluxes with the surrounding environment. This approach has been used to produce high-quality temperature estimation results with fine temporal resolutions (Brown, 1969; Sinokrot & Stefan, 1993; Beschta, 1997; D. Chen, Carsel, McCutcheon, & Nutter, 1998; Westhoff et al., 2007). However, such models call for data including meteorological conditions, channel geometry, land usage, and flow rate on a regular grid. Furthermore, the spatial extent of estimation is often limited. The full energy budget approach results

in a high computational burden. Because one of the main project goals is real-time information, the deterministic approach for a large domain, such as the entire state, with hourly computational updates does not serve as the best strategy.

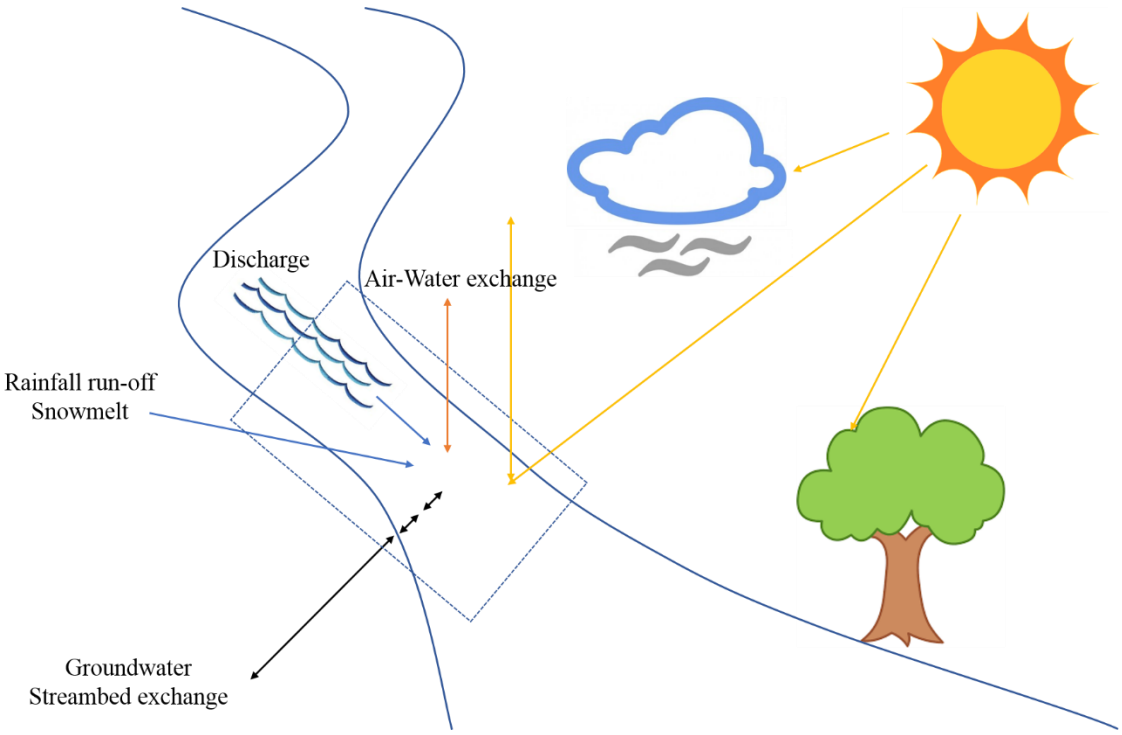

Figure 1.1 Illustration of physical factors influencing stream temperature in a control volume.

Among the four categories mentioned previously, atmospheric conditions are among the most dominant in affecting stream water temperature and are responsible for the heat exchange that occurs between the stream and the atmosphere. The source and sink term from Equation (1) accounts for the energy flux terms that are influenced by atmospheric conditions, and is formulated in Equation (2), where Q_{NR} is net radiative flux, Q_E is evaporative heat flux, Q_C is conductive heat flux, Q_H is convective heat flux, and Q_A is advective heat flux, which is often neglected.

$$S = Q_{NR} \pm Q_E \pm Q_C \pm Q_H \pm Q_A \tag{2}$$

The net radiation is composed of both shortwave and longwave radiation. The shortwave (solar) radiation, Q_{SR} can be expressed as

$$Q_{SR} = (Q_{Si} - Q_{So})(1 - SF) \tag{3}$$

where SF is the fraction of solar radiation blocked due to riparian vegetation (shading). The longwave radiation, Q_{LR} can be expressed as

$$Q_{LR} = \sigma(\varepsilon_w T_s^4 - \varepsilon_a T_a^4) \tag{4}$$

where T_s is the stream water temperature, T_a is the air temperature, ε_w is the emissivity of water surface, ε_a is the emissivity of the atmosphere, and σ is the Stefan-Boltzmann constant. The evaporative heat flux, Q_E can be expressed as

$$Q_E = 0.614U(e_{ws} - e_a) \tag{5}$$

where U is the wind speed, e_{ws} is the saturated vapor pressure at the stream temperature, and e_a is the atmospheric vapor pressure. The conductive heat flux, Q_C can be expressed as

$$Q_C = K(\frac{dT}{dz}) \tag{6}$$

where K is the thermal conductivity of the river bottom material and dT/dz is the temperature gradient in the river bottom. The convective heat flux, Q_H can be expressed as

$$Q_H = \frac{0.61P}{1000} Q_E \left[\frac{(T_s - T_a)}{(e_{ws} - e_a)} \right] \tag{7}$$

where P is the atmospheric pressure. The saturated vapor pressure can be expressed as

$$e_{ws} = 0.618 \exp(\frac{17.27T_s}{237.3 + T_s}) \tag{8}$$

Although a physics-based deterministic model provides a robust approach in which the performance is less limited by geographical features and hydrologic regimes, difficulty resides in the acquisition of all relevant meteorological data on a regular grid across a large domain. The computational burden would also be heavy and thus make it difficult to provide real-time hourly estimation updates.

This thesis employs a simple logistic regression modeling approach that builds on the air-water temperature relationship to produce state-wide stream temperature estimation with fine spatial and temporal resolutions and real-time updates. The simple statistical approach uses air temperature as the sole predictor, which is physically related to the longwave radiation, evaporative, and convective energy fluxes. The product is a widely and easily applicable model whose real-time state-wide output is visualized on the Iowa Water Quality Information System, Beta version (IWQIS Beta).

1.2 Literature Review

As one of the most influential parameters for aquatic habitat and river ecosystem health, river temperature has been modeled extensively over the past 50 years. Models of stream water temperature aim to ultimately result in more effective fisheries and nutrient growth management. Existing modeling approaches for stream water temperature simulation or prediction generally fall within three categories: deterministic, stochastic, and regression. Different techniques introduce different constraints on the spatial extent, spatial resolution, and temporal resolution of model estimation. The sections below provide an overview of the three types of modeling approaches as well as the benefits and drawbacks of each strategy.

1.2.1 Deterministic Models

River thermal regimes are highly influenced by meteorological and river conditions as well as by their geographical setting (Caissie, 2006). Deterministic models solve the full energy budget problem with respect to space and time through a partial differential equation. Equation (1) shown previously is an example of the model formulation developed by Sinokrot & Stefan (1993). The products usually provide high quality stream temperature estimations with fine spatial and temporal resolutions of within 1 to 2 ˚C (Brown, 1969; Sinokrot & Stefan, 1993; Beschta, 1997; D. Chen, Carsel, McCutcheon, & Nutter, 1998; Westhoff et al., 2007).

Although the deterministic modeling approach avoids making excessive assumptions about geographical settings, meteorological conditions, or river conditions, and is thus transferrable to basins of different sizes, it has a stringent data availability requirement. This approach requires all relevant meteorological data to calculate the energy flux components that affect river temperature. The models are computationally heavy as they integrate the partial differential equation with respect to both time and space. Therefore, spatial extents for deterministic model estimation often range from a segment of a first order stream (Westhoff et al., 2007) to the watershed level. However, deterministic models are well suited for impact studies as they consider the different energy fluxes and mixing zones within the river (Caissie, 2006). Studies on the impact of various factors, including streambed and groundwater heat fluxes, urbanization, and climate change, on stream temperature have been performed.

1.2.2 Stochastic Models

When compared to deterministic models which quantify the energy flux components experienced by the river, stochastic models are simpler as they require only air temperature as the input parameter. These models often separate water temperature time series into two components: the long-term annual component and the short-term component. The annual component captures the seasonal stream temperature change and can be represented using a Fourier series or a sinusoidal function (V. Kothandaraman, 1971; Cluis, 1972; Caissie, El-Jabi, & St-Hilaire, 1998; Caissie, St-Hilaire, & El-Jabi, 2004). The short-term component represents the departure of stream water temperature from the annual component. Air temperature data are used to model the short-term component, using methods including the Box and Jenkins method and the Markov process (Caissie, 2006). Stochastic models are often used for estimating stream temperatures at a daily temporal scale, and have been proven to provide good results of within 2 ˚C error. These models can be applied over large geographical areas with air temperature as the only available meteorological data, and they do not require high computational ability.

1.2.3 Regression Models

Compared to the two previous types of models, regression models are the least complex, and focus mainly on the relationship between water and air temperatures. Regression models are divided into three groups: linear, multiple, and logistic regressions. Similar to stochastic models, regression models can be applied over large

geographical areas with air temperature as the only input parameter. The computational ability require is low.

The linear regression method has been applied mostly to predict weekly or monthly data (Ficklin, Luo, Stewart, & Maurer, 2012). At relatively coarse temporal resolutions (e.g. weekly, monthly), the linear regression models generate satisfactory results (Ficklin et al., 2012). The multiple regression method incorporates a series of other explanatory variables on top of air temperature, such as solar radiation, discharge, and time lag. These models usually employ a suite of parameters to predict stream temperature (Jeppesen & Iversen, 1987; Jourdonnais, Walsh, Pickett, & Goodman, 1992).

Studies have found that the air-water relationship changes with the temporal resolution (Caissie, 2006). For finer resolutions (e.g. daily, hourly), a significant departure from linearity in the water–air temperature relationship was observed (O. Mohseni & Stefan, 1999; Webb, Clack, & Walling, 2003). O. Mohseni and Stefan (1999) explained that due to groundwater influences at low air temperature and evaporative cooling at high air temperature, linear extrapolations to high and low air temperatures are not justified. Comparatively, logistic regression better captures non-linearity in the water-air temperature relationship.

This nonlinear logistic regression approach was first used for stream temperature modeling by Omid Mohseni, Stefan, and Erickson (1998). The logistic function formulated as Equation (9) was selected to fit the S-shaped function relationship between water and air temperatures as it is the most stable function and its parameters possess physical meanings.

Chen and Fang (2015) employed simple methods, including linear, polynomial, and logistic regressions, to estimate hourly water temperatures in rivers in Alabama, and they applied the models to eight rivers in and outside the region. They found that logistic regression models outperform linear models in hourly stream temperature estimations. Meanwhile, Segura et al. (2015) provided a summary of the regression models derived at hourly, daily, weekly, and monthly scales for different spatial extents, using mostly linear and logistic functions. They also found that logistic regression is the better adapted approach of the three commonly used regression methods to estimate stream temperature at fine temporal resolutions (e.g. daily, hourly). The logistic regression approach has thus been favored for the last few decades (Omid Mohseni et al., 1998).

One commonly included parameter in regression models is the lag time between daily air and water temperature peaks, often referred to as the shift parameter. Rutherford et al. (2004) found that for small streams, water temperature typically takes about 4 hours to reach dynamic equilibrium, despite the shading effect. Chen and Fang (2015) also found the time lag to be typically on the order of 4 to 5 hours for the eight rivers in Alabama. Regression models are often developed separately for every season. Segura et al. (2015) explained that not only the stream thermal sensitivity, but also the mean stream temperatures change seasonally. Hence regression parameters that capture the air-water relationship are fitted separately for each season. The winter season is often excluded as the annual temperature cycle typically spans from spring to autumn. Freezing and thawing processes during winter introduce separate energy components that destroy the temperature relation.

1.2.4 Parameters Neglected by Regression Models

Compared to full energy budget deterministic models, regression models lack the ability to simulate stream temperature variations due to parameters such as solar radiation, groundwater and streambed heat fluxes, riparian shading, and anthropogenic perturbations. Studies were thus performed to quantify and compare heat fluxes and their resultant percentage variability in water temperature.

Evans, McGregor, and Petts (1998) found that over 82% of the total energy flux occurred at the air–water interface and about 15% at the channel bed. Additionally, Sinokrot and Stefan (1994) found through sensitivity analysis that streambed heat flux only accounts for within -0.12 to +0.15 °C of stream temperature variability. However, the effect can become more significant for small streams of less than 3 meters in length (Caissie, 2006). Younus, Hondzo, and Engel (2000) found that solar (shortwave) radiation and subsurface inflow are the most significant contributors to the stream heat budget through modeling for an upland agricultural watershed located in Indiana for every 15 minutes over 25 days. Sinokrot and Stefan also stated that streambed heat fluxes are more important for hourly stream temperature estimations (1993). Therefore, errors in hourly stream temperature estimations using regression models can be due, in no small part, to these unaccounted-for energy fluxes.

A few other physical factors not included in the regression models can influence the stream thermal regimes and ecosystems, and further influence the ecological processes and stream biota. For example, cumulative stream temperature dynamics depend on upstream heat accumulation and groundwater inputs (Kelleher et al., 2012), which are influenced by land cover characteristics and urbanization (Nelson & Palmer,

2007). Solar radiation and wind are reduced with the increase in riparian vegetation coverage. As a canopy reduces solar radiation influx as well as the escape of energy due to wind, the effects of the two components may cancel out each other and lead to a stronger air-water temperature relationship. Rutherford, Marsh, Davies, and Bunn (2004) also found that the shading effect on stream water temperature only applies over short distances and travel times. The effect can be neglected for larger streams.

Anthropogenic perturbation influences are important for environmental assessment and modeling. Nelson and Palmer stated that "multiple anthropogenic stressors, including increased watershed imperviousness, destruction of the riparian vegetation, increased siltation, and changes in climate, will impact streams over the coming century" (2007). These stressors further complicate the modeling problem. For example, Nelson and Palmer (2007) found that land use alteration has an obvious impact on the daily average stream temperatures by creating surges of as large as 7 °C. The impacts could be especially significant for low flow sites. Hence urban streams experience temperature surges that need to be better quantified.

Precipitation, as another source of inflow, can also affect stream temperature. High runoff precipitation events were found to cause stream temperature surges of about 3.5 °C, which dissipate over about 3 hours (Nelson & Palmer, 2007). The surges are especially noticeable in the summer at urban areas. Simple regression models fail to quantify such surges.

1.2.5 Other Modeling Strategies

Novel modeling strategies that fall outside of the three main categories exist. Chen and Fang (2015) developed and evaluated a modified wave function model based on the logistic regression approach and produced hourly water temperature estimations for eight major rivers in Alabama. They proved that the modified wave function model provides better results (NS for most rivers exceeding 0.90) than the direct linear and non-linear regression models. With the advancement in soft computing technologies, artificial neural networks (ANNs) have been increasingly applied to hydrologic modeling over the last decade. Chenard and Caissie (2008) utilized ANNs to develop a daily maximum and mean stream temperature estimation model for a small drainage basin. The approach provided equally good results as the conventional modeling techniques, while presenting certain advantages, such as simplicity of use.

1.2.6 Summary

Current models vary on the estimation resolution, both temporally and spatially. The estimation duration and spatial extent can also be limited by the modeling approach. The EPA (2016) states that "moving average metrics such as 7-day mean and maximum are useful descriptors of thermal regimes and often associate well with stream fish distribution patterns." Stella (2013) also states that daily maximum and minimum temperatures are sufficient in assessing fish habitat distributions. Hence most of the previous studies construct models to predict or estimate stream temperature for individual river/reach with relatively coarse time resolutions (e.g. daily, weekly, monthly, seasonal, and annual). However, higher temporal resolution is useful for nutrient growth modeling.

An example of a fine resolution model was presented in Westhoff et al. (2007), as the stream temperature was simulated at 2-minute and 1-meter resolutions for a 1,500-meter reach spanning one week.

CHAPTER 2 METHODOLOGY

2.1 Introduction

For this thesis, a real-time hourly stream temperature estimation model that is available on any arbitrary stream/river segment in the state of Iowa was developed, evaluated, and implemented. The procedures conducted to achieve this product were site-specific model development, state-wide integration, and real-time implementation. This chapter documents the data acquisition, management, and preservation processes, as well as the site-specific statistical model development methodology.

2.2 Project Scope & Available Data

This project's statistical model development and evaluation used historical water temperature measurement data from the United States Geological Survey (USGS) and IIHR-Hydroscience & Engineering (IIHR), as well as historical air temperature measurement data from the National Oceanic and Atmospheric Administration (NOAA). In order to capture the diurnal characteristic of water and air temperatures, hourly data resolution is required for both data records. Meanwhile, relative changes in stream temperature and model performance due to instream flow alterations were of interest. Hence hourly/sub-hourly stream discharge rate measurements from the USGS sites were acquired upon availability. Locations of the water and air temperature measurement stations within the state of Iowa are shown in Figure 2.1.

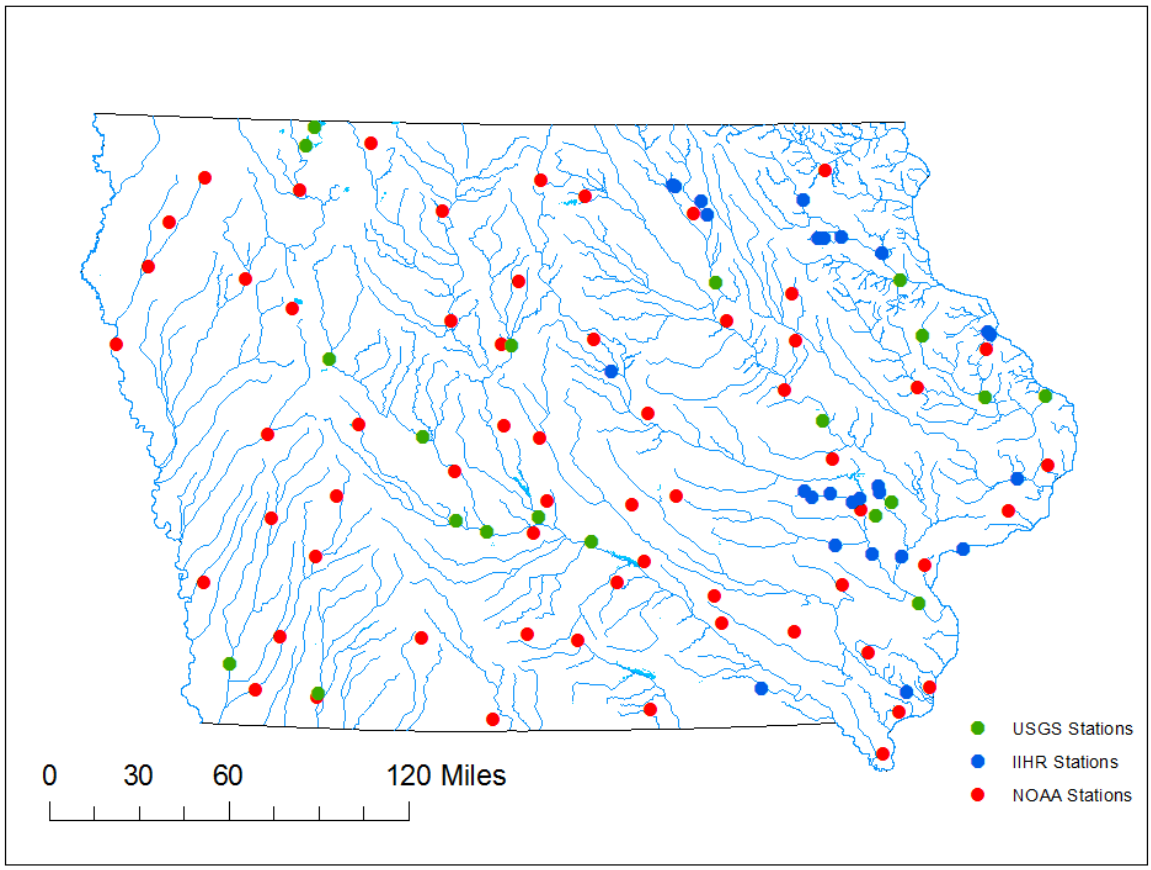

Figure 2.1 Iowa USGS, IIHR, and NOAA sites that provide hourly/sub-hourly water and air temperature measurements (Iowa Department of Natural Resources and Iowa Geological Survey, 2017).

Twenty USGS stream gages in the state of Iowa are utilized in this project. Drainage area sizes ranging from 7.1 to 32,375 square kilometers (2.76 to 12,500 square miles) were used for model development, shown in Table 2.1. Additionally, there are 25 sensors among the IIHR Water-Quality Monitoring Network that provide sub-hourly water temperature measurements, in light of IIHR's water-quality initiative. The drainage area sizes range from 7.77 to 20,168 square kilometers (3 to 7,787 square miles), shown in Table 2.2. The sensors with at least one year of recorded data are used for model development and evaluation. Although the exact start and end dates of the data recording period at each site vary, the earliest available sub-hourly water temperature

measurements from both USGS and IIHR start from the year 2012. A majority of the USGS sites selected provide hourly/sub-hourly discharge measurements, allowing for studies on the discharge-temperature relationship and model sensitivity analyses.

Comparatively, NOAA has a denser population of stations located throughout the state that provide air temperature measurements. The Automated Weather Observing System (AWOS) and the Automated Surface Observing System (ASOS) networks together have 60 stations that record hourly/sub-hourly air temperature measurements, starting long before the water temperature measurements were available. Information on the 60 NOAA stations is shown in Table A-1. Each water temperature measurement site is paired with the most adjacent air temperature measurement station to provide data for the statistical model. The pairing information for NOAA stations and USGS and IIHR sites is shown in Table 2.1 and 2.2, including the distance in-between stations, which ranges from 2.23 to 58.4 kilometers (1.39 to 36.3 miles).

Table 2.1 USGS water temperature measuring stream gage (USGS, 2017) and pairing NOAA air temperature station information.

USGS Site ID	Drainage Area (km^2)	Latitude	Longitude	Start Date	End Date	NOAA Site ID	Distance in between (km)
0546494205	7.15	41.67	-91.34	16-Mar	16-Dec	IOW	16.96
06604000	195.8	43.47	-95.12	11-Oct	16-Dec	EST	31.3
05418110	316	42.47	-91.12	12-Apr	14-Nov	MXO	28.0
06604200	324	43.38	-95.18	11-Oct	16-Dec	SPW	23.5
05455100	521	41.61	-91.45	12-Feb	15-Nov	IOW	8.77
05418400	1308	42.16	-90.73	12-May	14-Nov	DBQ	26.1
05482300	1813	42.35	-94.99	12-Mar	16-Dec	SLB	33.9
06817000	1974	40.74	-95.01	12-Sep	16-Dec	ICL	2.23
05481000	2186	42.43	-93.81	12-Mar	16-Dec	EBS	5.27
05484000	2445	41.59	-94.15	16-Feb	16-Dec	PRO	26.5
06808500	3434	40.87	-95.58	16-Mar	16-Dec	SDA	19.47
05412500	4002	42.74	-91.26	12-May	16-Dec	MXO	58.4
05458300	4007	42.74	-92.47	11-Oct	16-Dec	ALO	21.1
05482500	4193	41.99	-94.38	12-Mar	16-Dec	PRO	25.1
05418720	4841	42.16	-90.34	14-May	16-Dec	CWI	37.2
05484500	8912	41.53	-93.95	12-Mar	16-Dec	DSM	24.7
05482000	16174	41.61	-93.62	13-Sep	16-Dec	DSM	9.14
05464420	16426	42.07	-91.79	12-Oct	16-Dec	CID	21.3
05487520	30303	41.49	-93.28	11-Oct	16-Dec	OXV	25.4
05465500	32375	41.18	-91.18	11-Oct	16-Dec	MUT	21.3

Table 2.2 IIHR water temperature measuring water quality sensor and pairing NOAA air temperature station information.

IIHR Site ID	Drainage Area (km^2)	Latitude	Longitude	Start Date	End Date	NOAA Site ID	Distance in between (km)
1	8151	41.69	-91.55	12-Sep	15-Dec	IOW	6.06
2	254	41.68	-91.60	12-Jun	15-Dec	IOW	6.08
3	158	41.72	-91.74	12-Jun	15-Dec	CID	18.35
4	20.7	41.70	-91.86	12-Jun	14-Dec	CID	23.0
5	1492	41.47	-91.71	12-Apr	15-Dec	AWG	21.9
6	11119	41.42	-91.48	12-Jun	15-Dec	AWG	23.3
7	20168	41.41	-91.29	12-Jun	14-Dec	MUT	13.37
8	15.54	43.21	-92.75	13-Sep	15-Dec	CCY	18.86
9	119.1	42.95	-91.64	13-Jun	15-Dec	DEH	36.8
10	11168	40.75	-91.28	13-Oct	15-Dec	FSW	11.06
11	25.9	41.73	-91.91	14-Apr	15-Dec	CID	22.7
12	12.95	43.21	-92.73	14-May	15-Dec	CCY	17.69
13	44.0	43.07	-92.53	14-May	15-Dec	CCY	6.93
14	18.13	43.13	-92.57	14-May	15-Dec	CCY	7.75
15	67.3	42.95	-91.75	15-Apr	15-Dec	OLZ	34.8
16	38.8	42.95	-91.80	14-Apr	15-Dec	OLZ	32.9
17	20.7	43.13	-91.89	14-Jul	15-Dec	DEH	19.75
18	300	42.87	-91.38	14-Jul	15-Dec	OLZ	52.9
19	80.3	40.78	-92.20	14-Apr	15-Dec	FFL	34.9
21	15.54	41.72	-91.43	14-Oct	15-Dec	IOW	13.42
22	7.77	41.75	-91.43	14-Oct	15-Dec	IOW	15.21
23	6050	41.77	-90.54	15-Apr	15-Dec	DVN	17.78
24	580	42.31	-93.15	15-Apr	15-Dec	IFA	19.48
25	106	42.47	-90.68	15-Apr	15-Dec	DBQ	7.97
26	33.7	42.48	-90.70	15-Apr	15-Dec	DBQ	9.29

Quality assurance and quality control as well as simple sampling strategies were performed on the raw data acquired from USGS, IIHR, and NOAA. The formatted annual data files contain quality controlled, continuous hourly data measurements of water temperature, discharge, and air temperature. Raw data files contain missing data, non-unified time zones, and occasional unreasonable temperature values, such as air temperature readings of above 50 °C. A maximum threshold of 48 °C was set for air temperature according to the historical highest recorded at July 20, 1934 in the state of Iowa (NOAA, 2017a). A minimum threshold of -0.1 °C was set for water temperature to indicate freezing conditions. Any recorded value that did not meet the set thresholds was treated as missing data. All data were transformed into Coordinated Universal Time (UTC). The raw and modified data, as well as the data manipulation scripts were preserved on the IIHR network storage.

2.2 Model Development

The water-air temperature relationship that the statistical model is built on is captured by a four-parameter logistic function, shown as:

$$T_s = \mu + \frac{\alpha - \mu}{1 + e^{\gamma(\beta - T_a)}} \tag{9}$$

Figure 2.2 is a graphical representation of the logistic function. The four parameters in the logistic function each corresponds to: historical maximum water temperature in ˚C (α), historical minimum water temperature in ˚C (μ), steepest slope of the function at the inflection point (γ), and air temperature at the inflection point in ˚C (β).

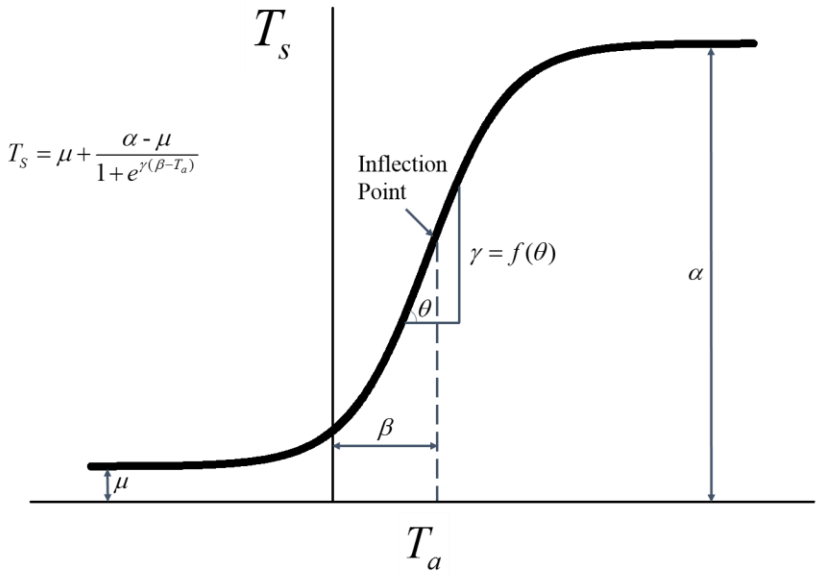

Figure 2.2 Logistic relationship between water and air temperatures.

An example scatter plot of the two temperatures is shown in Figure 2.3. The summer 2015 hourly water temperature measurements at USGS station 05412500 on the Turkey River at Garber, IA (hereafter as the Turkey River site) and the pairing hourly air temperature measurements from NOAA station MXO were plotted. The logistic relationship is especially evident as the lower and upper tails approach the threshold asymptotes.

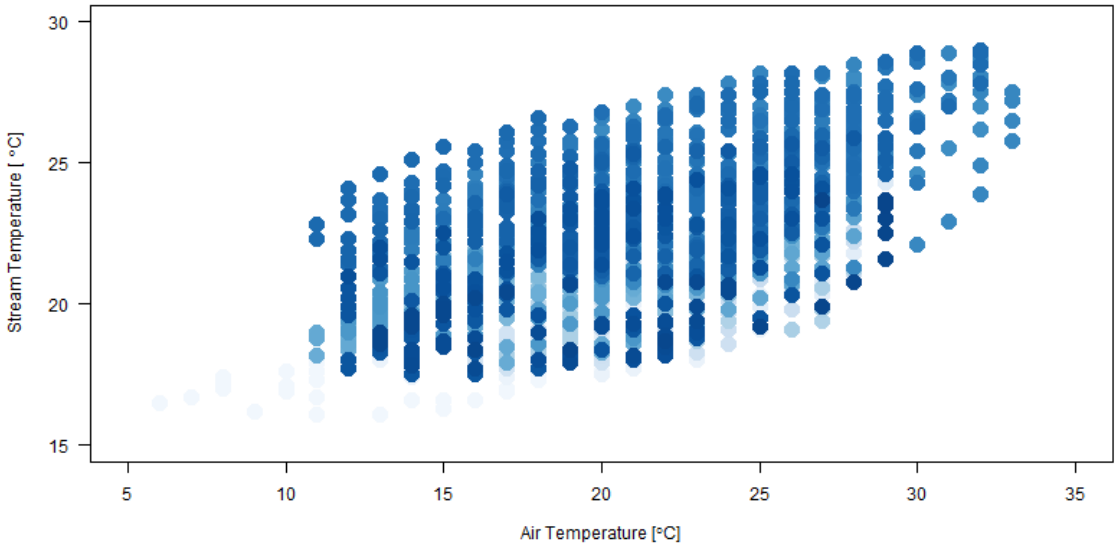

Figure 2.3 Scatter plot of stream temperature versus air temperature for summer 2015 at the Turkey River site. Warmer colors indicate higher density of points.

The maximum and minimum water temperature values (α and μ) are easily established from the measurement data for each station and period of interest. These two parameters set the upper and lower bounds for water temperature estimations. The remaining two model parameters (γ and β) use regression fitting procedures. There are two computational methods developed for this task. One method is referred to as the Logit method, and the other is referred to as the gridded iteration method.

The Logit method estimates γ and β values by transforming Equation (9) into a linear function in the form of:

$$y = a_0 x + a_1 \tag{10}$$

with the independent variable being air temperature, and the dependent variable being $-\log(\frac{\alpha-\mu}{T_s-\mu}-1)$ (also known as $Logit_y$), calculated using water temperature data. The linear function parameters a_0 and a_1 are estimated using Equations (11) through (18),

where *n* is the number of available hourly water and air temperature measurement pairs in the period.

$$a_1 = \frac{n * sum_{xy} - sum_x * sum_y}{n * sum_{x^2} - (sum_x)^2} \tag{11}$$

$$a_0 = y_m - a_1 x_m \tag{12}$$

$$sum_x = \sum T_a \tag{13}$$

$$sum_y = \sum Logit_y \tag{14}$$

$$sum_{xy} = \sum T_a * Logit_y \tag{15}$$

$$sum_{x^2} = \sum T_a{}^2 \tag{16}$$

$$x_m = \frac{\sum T_a}{n} \tag{17}$$

$$y_m = \frac{\sum Logit_y}{n} \tag{18}$$

The logistic regression model parameters γ and β are then calculated from the linear function parameters, using Equations (19) and (20).

$$\gamma = a_1 \tag{19}$$

$$\beta = \frac{-a_0}{\gamma} \tag{20}$$

The second approach, which is the gridded iteration method, performs optimization through a systematic search on a regular grid to estimate γ and β values. Step sizes of 0.01 and 0.001 were set to be the grid resolution for the search of γ and β values. Values are found as the parameter pair that provides the least root mean square

error (*RMSE*) between the observed and estimated stream temperature. This method requires more computational time than the previous approach. However, the Logit method finds logistic function parameter values by achieving the least squares error on the transformed linear function dependent variable. Therefore, despite the higher computational burden, the gridded iteration method is the better approach as it finds parameter values through optimization on the actual stream temperature estimation. The gridded iteration method was thus selected for the statistical model development.

The summer 2015 time series plot of hourly stream and air temperature measurements at the Turkey River site is shown in Figure 2.4. Strong seasonal cycles are observed in both temperatures. Due to such behavior, the model was fitted separately for each season of interest. Both biotic and abiotic processes occur at minimum rates in low-temperature environments. As a result, prediction of stream temperature around freezing is not of main interest. Literature also shows that stream and air temperatures lose the logistic relationship in the winter season (Caissie, 2006). Therefore, the model was developed to estimate stream temperature in three seasons separately: spring (March to May), summer (June to August), and autumn (September to November). Summer exhibits the strongest logistic relationship between the two temperatures as the streambed and groundwater heat fluxes become relatively insignificant compared to the longwave radiation, latent heat, and sensible heat fluxes.

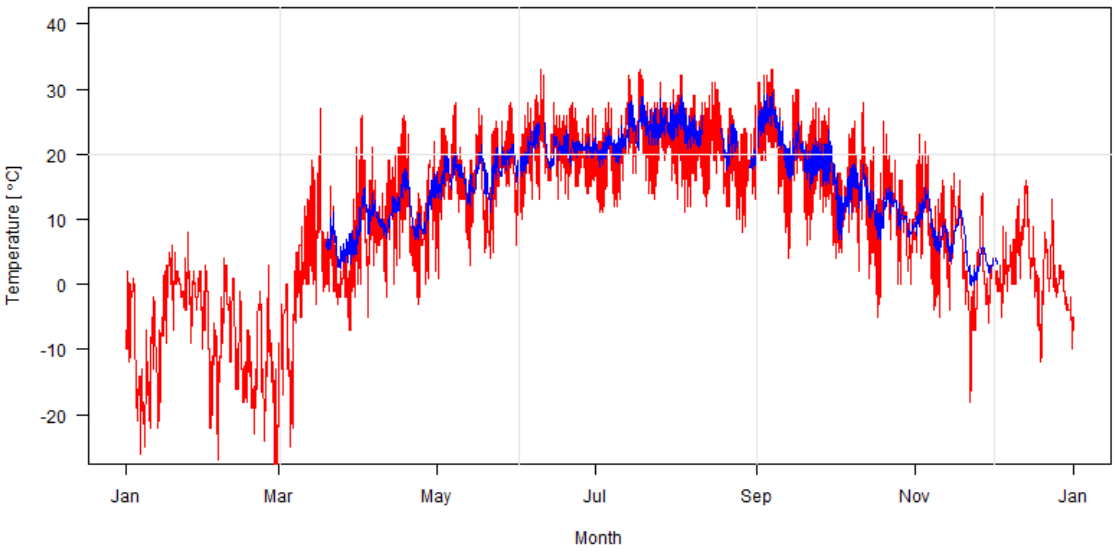

Figure 2.4 2015 hourly water and pairing air temperature measurements at Turkey River site. Blue: steam temperature. Red: air temperature.

Stream and air temperatures both exhibit sinusoidal behavior. Stream temperature usually spans smaller amplitudes than air temperature. Besides the strong seasonal cycle, both temperatures follow the diurnal cycle. The July 2015 time series of the stream and air temperature measurements at the Turkey River site offers a zoomed-in view of the diurnal temperature behavior. The sinusoidal waves of the two temperatures, as shown in Figure 2.5, are not entirely in phase with each other. A constant time lag exists between the stream and air temperatures. The lag is existent for every site regardless of the geological location and season, and is due largely to the specific heat variation between water and air. 24 hourly temperature averages were taken using the summer period data to evaluate the diurnal-average peak time difference. It was found that water temperature, on average, reached peak value 3 hours later than air temperature in summer 2015 at the Turkey River site.

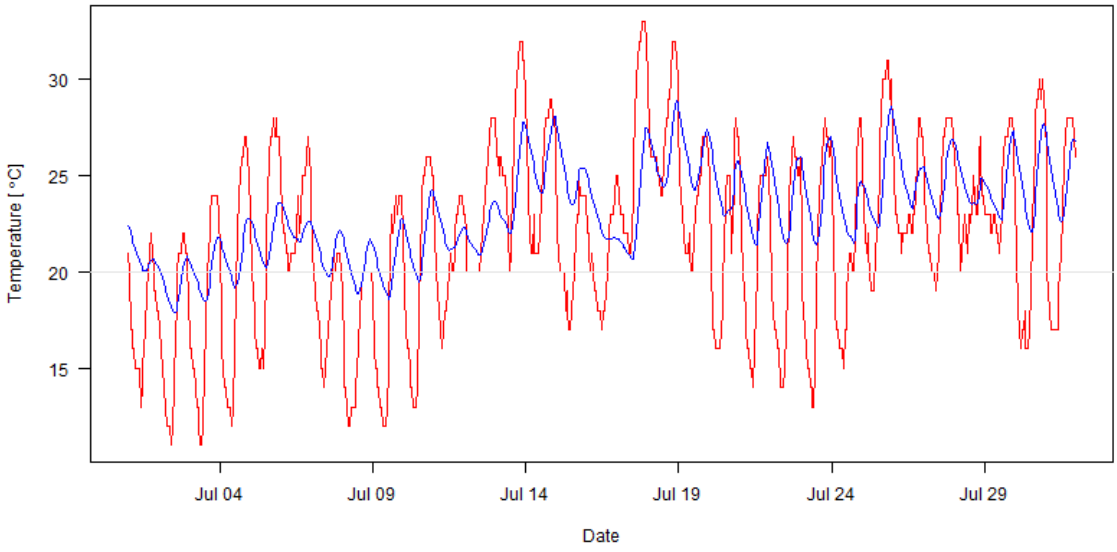

Figure 2.5 July 2015 hourly water and pairing air temperature measurements at the Turkey River site.

The time lag between stream and air temperatures was included in the model as an additional parameter named shift. The incorporation of shift enhances the logistic relationship by shifting the temperature datasets. The gridded iteration process was performed using stream temperature measurements promoted by discrete hour amounts of 0 to 8. The optimum shift value maximizes the predictive relationship between the two temperatures and is determined through the least squares error method. Hence the modified logistic regression equation takes the final form of:

$$T_s(t) = \mu + \frac{\alpha - \mu}{1 + e^{\gamma(\beta - T_a(t - shift))}} \quad (21)$$

Final logistic parameter values for each site and season were set to be the estimated values for the temperature dataset corresponding to the optimum shift hour. The model development scripts were preserved on the IIHR network storage as well.

2.3 Chapter Summary

Each USGS and IIHR water temperature measurement location was paired with the most adjacent NOAA air temperature measurement station for acquisition of data for the spring, summer, and autumn seasons. Every seasonal dataset of hourly water and air temperature measurements was fitted using the logistic regression to develop site-specific seasonal models. The regression model incorporates an extra parameter, which is the lag time between stream and air temperature peaks, to enhance the logistic relationship.

Of the four logistic regression parameters, α and μ were found as the maximum and minimum stream temperatures within the dataset, γ and β were found using the least squares error method through a systematic search on a regular grid. Grid steps of 0.01 and 0.001 for γ and β were employed. The logistic relationship between the two temperatures was enhanced with the incorporation of the shift parameter. The optimum shift value was estimated with a search from 0 to 8 hours and is used to provide the final estimated logistic parameter values to achieve minimum estimation error.

The model fitting process takes, on average, around 3 minutes to generate parameter values and hourly stream temperature estimations for each seasonal dataset. All original and modified data, as well as the data manipulation and model development scripts, were preserved on the IIHR network storage.

CHAPTER 3 MODEL EVALUATION

3.1 Introduction

As described in the previous chapter, the statistical stream temperature estimation model was developed for water temperature measurement-available sites. The estimated model parameter values were used to produce hourly stream temperature estimations for the same seasonal dataset using the hourly air temperature measurements as input. The model estimation root-mean-square-errors (RMSEs) were calculated and used as the standard parameter for estimation error. Explanatory analyses were performed to study error behavior, and justify the model adequacy in its state-wide implementation. The analyses carried include sensitivity analyses, conditional error analyses, and outlier analyses. Model performance for the reservoir cases were also investigated to justify the model assumption of reservoirs and lakes as regular stream reaches. Additionally, a simple energy budget calculation was done for the first day of August at a sample location to quantify the percentage of shortwave radiation in total energy flux that the model does not account for. The model evaluation analyses and results for the site-specific regression model are documented in this chapter.

3.2 Evaluation Criterion

The threshold for good model performance was tentatively set to a seasonal model estimation root-mean-square-error (RMSE) of within 2 °C. This threshold has been used by other studies as a standard for good modeling results (Caissie, 2006). Nutrient growth activities, such as algal blooms, which are rapid growth events of microscopic algae or

cyanobacteria in water, require “warm” stream temperature environments. As a commonly used thermal threshold for nutrient growth monitoring models, 20 ˚C sets a value for which the temperatures above indicate accelerated nutrient survival and growth rates. Therefore, the model prediction is of most interest when the stream temperature exceeds 20 ˚C, which generally occurs from May to September in Iowa. Hence evaluation mainly focuses on the summer season model performance.

During the summer of 2015, 80.2% of the stream temperature measurements exceed 20 ˚C at the Turkey River site. The stream and air temperature measurements, as well as the regression model estimations are shown in Figure 3.1 (a). The model estimation RMSE is 2.04 ˚C. As observed, the logistic function captures the general trend and shape of the temperature observations. However, the additive errors between the measured and estimated stream temperatures can become quite large.

Comparatively, by altering the dataset using the optimum shift value, Figure 3.1 (b) displays the resultant temperature measurements and model estimations. Through promoting the stream temperature measurements by 4 hours, the model estimation RMSE was improved to 1.69 ˚C. The scatter points exhibit a stronger logistic relationship, reducing the additive errors between the measured and estimated temperatures. Note that although the RMSE was improved by only 0.35 ˚C, the amount is still considerable due to the 2 ℃ error requirement. The 2015 summer and July stream temperature estimation time series (using 4 hours of shift) in comparison with the observation data are shown in Figure 3.2 and Figure 3.3, respectively. It appears that the model captures the amplitudes of the diurnal cycles well. However, it can fail at capturing the observed daily maximum or minimum temperatures.

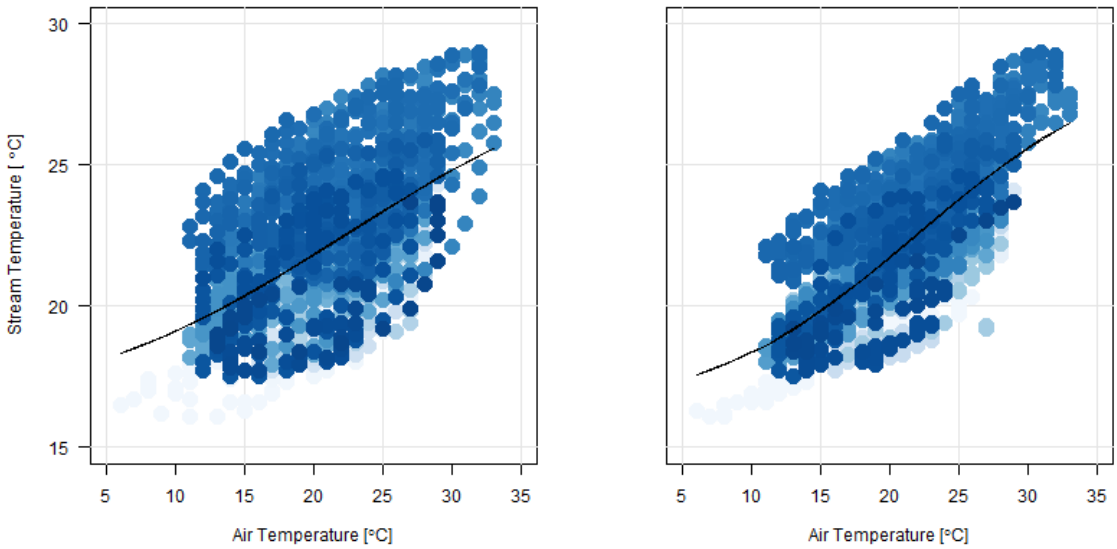

Figure 3.1 Scatter plots of stream temperature versus air temperature with regression lines for summer 2015 at the Turkey River site. Black continuous lines indicate the fitted logistic regressions. (a): without shift (RMSE = 2.04 ˚C); (b): with 4-hour shift (RMSE = 1.69 ˚C).

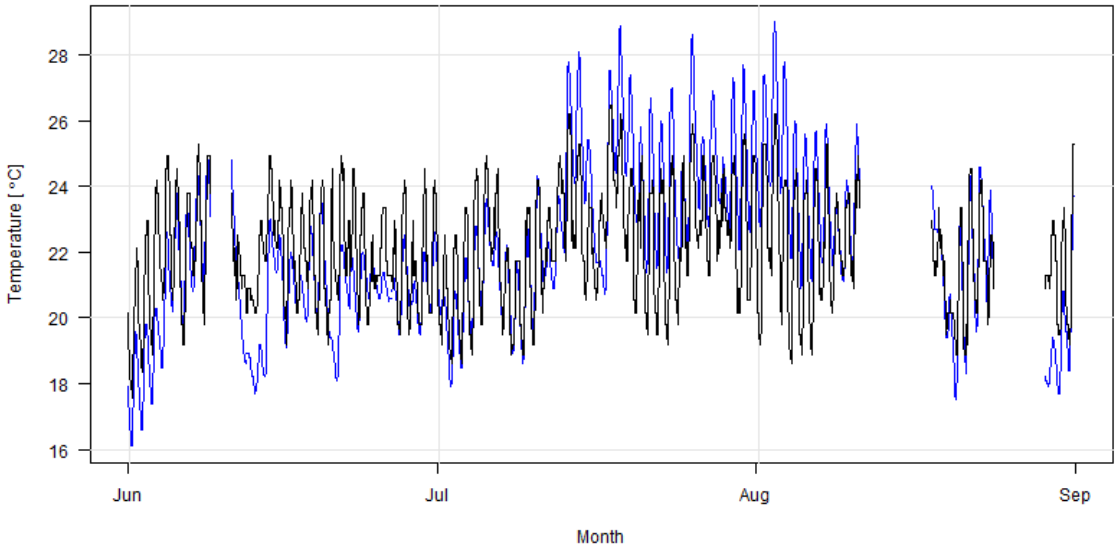

Figure 3.2 Summer 2015 stream temperature hourly observations and estimations at the Turkey River site. Blue: hourly observed stream temperature. Black: hourly estimated stream temperature.

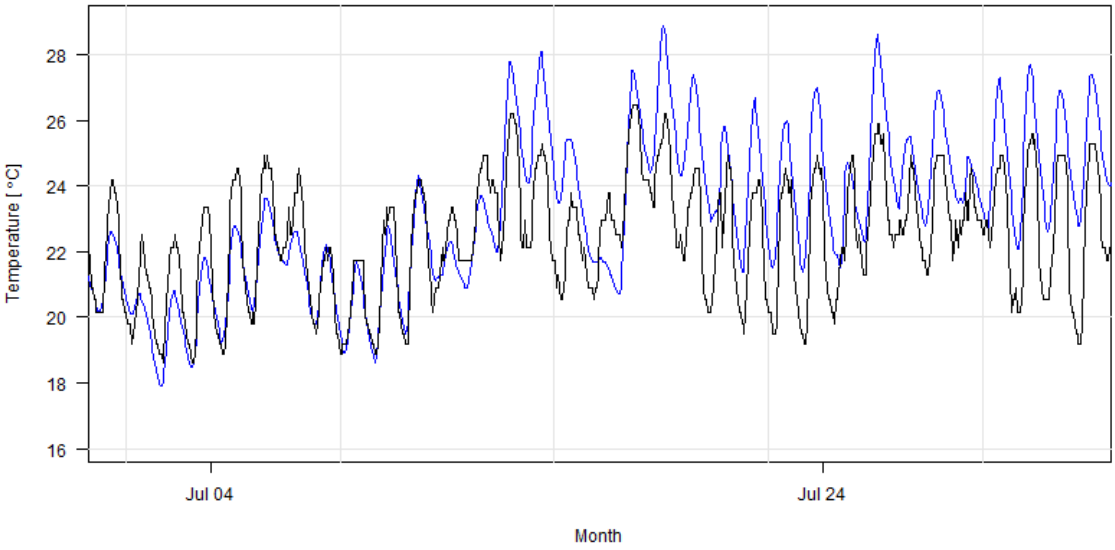

Figure 3.3 July 2015 stream temperature hourly observations and estimations at the Turkey River site. Blue: hourly observed stream temperature. Black: hourly estimated stream temperature.

3.3 Sensitivity Analysis

A series of sensitivity analyses were performed to examine how the model performance responds to changes in different variables. The model estimation RMSEs for spring, summer, and autumn of every data-available year at every site appear in Tables A-2, A-3, A-4 in the Appendix. The analyses were conducted to provide insight on patterns in the statistical model performance. All analyses were done for seasonal datasets with more than 1000 pairs of valid hourly water and air temperature measurements to account for the effect of missing data on model performance. As stated previously, most analyses results shown are for the summer season datasets as it is the period of most interest with frequent in-stream biological and chemical activities. Spring and autumn season data have similar characteristics as summer, but display a wider range of temperature variability.

3.3.1 Model Performance and Flow

When considering the energy budget, water quantity plays a major role in affecting stream water temperature behavior as it directly relates to the thermal inertia of the water body. Moreover, low or high flow conditions are important to fish habitat studies, and can alter the river thermal regimes. However, the statistical model developed in this thesis does not account for the impact of flow quantity on stream temperature. Thus the correlation between hourly discharge amount and stream temperature, as well as the impact of areal normalized discharge on the overall model performance, were studied.

A majority of the USGS sites that measure stream temperature also record hourly discharge measurements. Hourly discharge and stream temperature values were plotted for the summer of 2015 at the North Raccoon site, as shown in Figure 3.4. No predictive relationship was observed between the two variables. Hence the conclusion arrived at was, although the amount of water in-stream can have an impact on the overall river thermal regime, the hourly discharge amount does not correlate well with the hourly stream temperature.

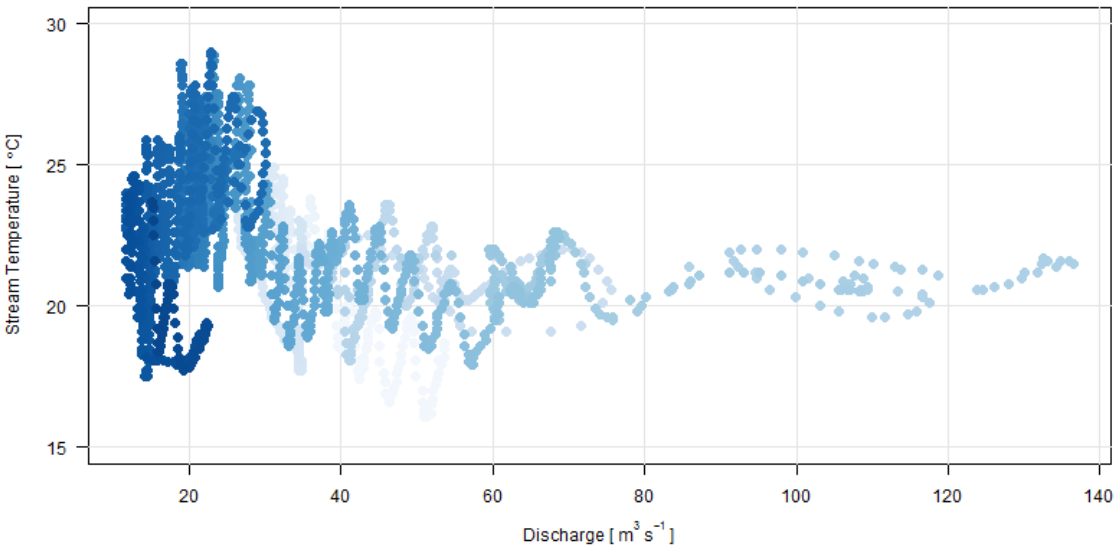

Figure 3.4 Scatter plots of stream temperature versus discharge for summer 2015 at the North Raccoon site.

To further study the relationship between model performance and the flow quantity in rivers, the RMSEs for all datasets were compared against the areal normalized discharge values (average seasonal discharge values divided by drainage area sizes). This analysis gives insight into how the model responds to change in the relative quantity of discharge. Figure 3.5 shows the scatter plot of the two variables, where no direct relationship was observed. Similarly, Figure 3.6 shows the summer season model RMSEs versus areal normalized discharge values. Linear regression test statistics indicate that only 6% of the variability in model estimation RMSE could be explained by areal normalized discharge for all datasets, and about 3% explained for the summer season. This result is conceivable as the increase in discharge results from an aggregation of source water, for which the temperature has already been related to the air temperature upstream. Furthermore, air temperature does not have much variation in space, so the change in discharge does not affect model performance distinctly.

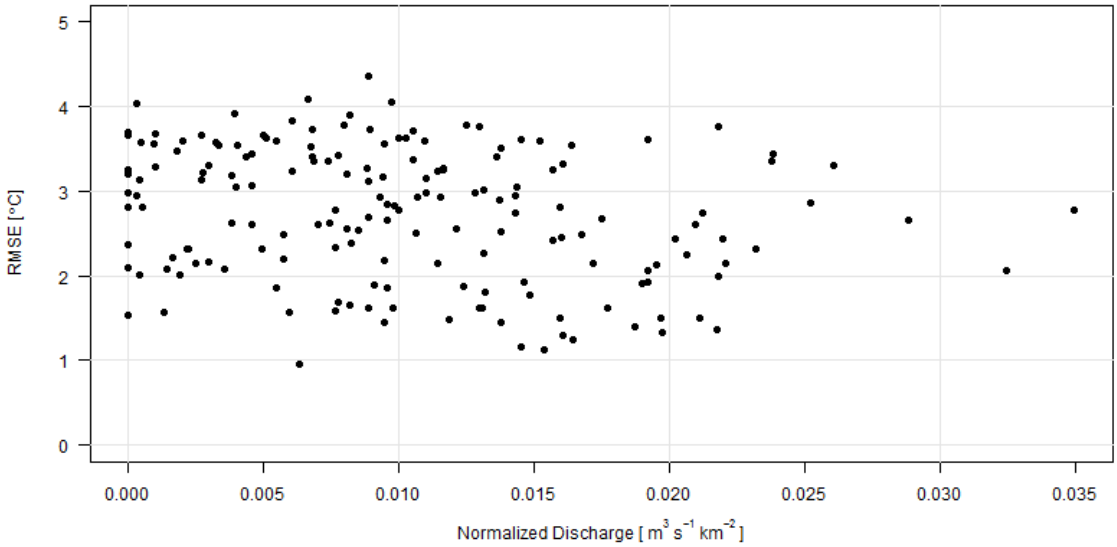

Figure 3.5 Model RMSE versus normalized discharge for all datasets (R^2 = 0.058).

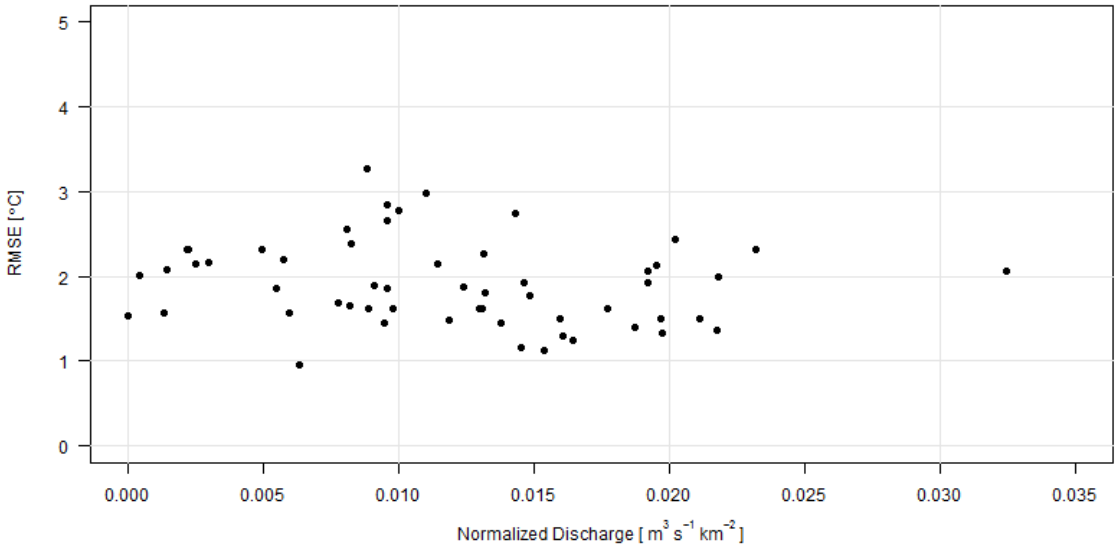

Figure 3.6 Model RMSE versus normalized discharge for summer season datasets (R^2 = 0.03).

3.3.2 Model Performance and Drainage Area

This analysis focuses on the impact of the drainage area size on model performance, to provide insight into how the model performs with changes in the size of

the stream. Linear regression was fit between the model estimation RMSE and drainage area size for every seasonal dataset. Figure 3.7 shows the summer season scatter plot. As observed in the graph, the IIHR sites tend to cover smaller rivers, whereas USGS sites span a wider range of river sizes. There is no strong correlation detected between the two variables. Test statistics show that the drainage basin size explains only about 0.8% of the variability in model estimation error. For spring and autumn seasons, drainage basin size explains about 24.7% and 24.0% of the variability in model estimation error, respectively (Figure 3.8 and Figure 3.9). Although the coefficient of determination is higher for spring and autumn, only 6.8% of the variability in RMSEs for all datasets could be explained by drainage area size (Figure 3.10).

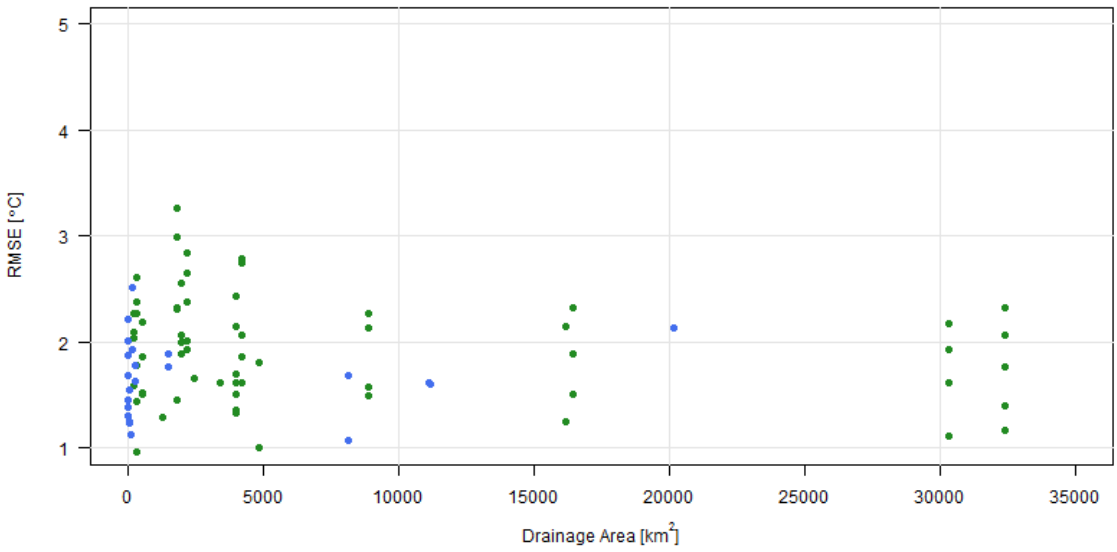

Figure 3.7 Model RMSE versus drainage area size for summer season datasets (R^2 = 0.008). Green: USGS data. Blue: IIHR data.

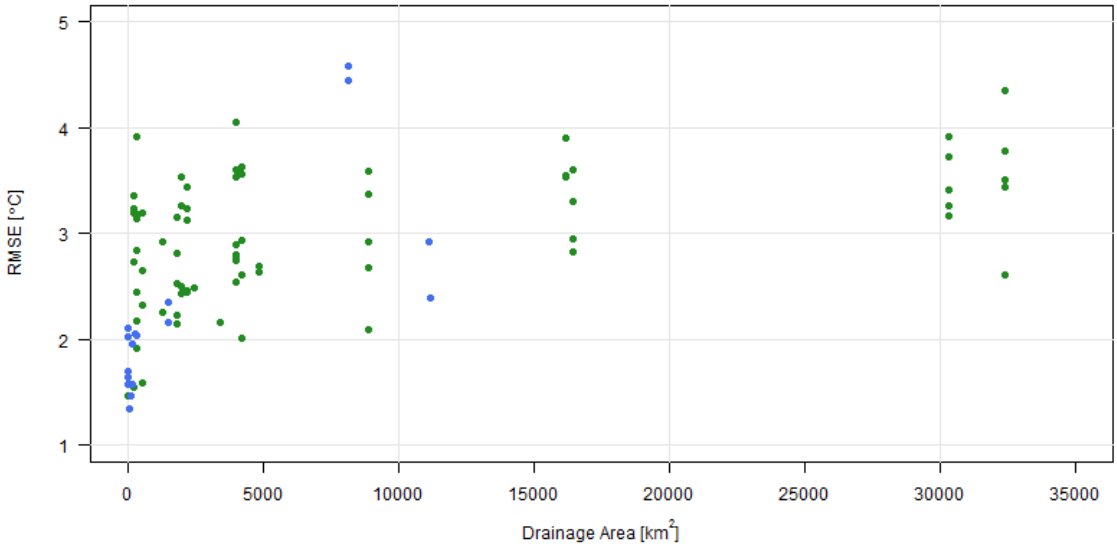

Figure 3.8 Model RMSE versus drainage area size for spring season datasets (R^2 = 0.247).

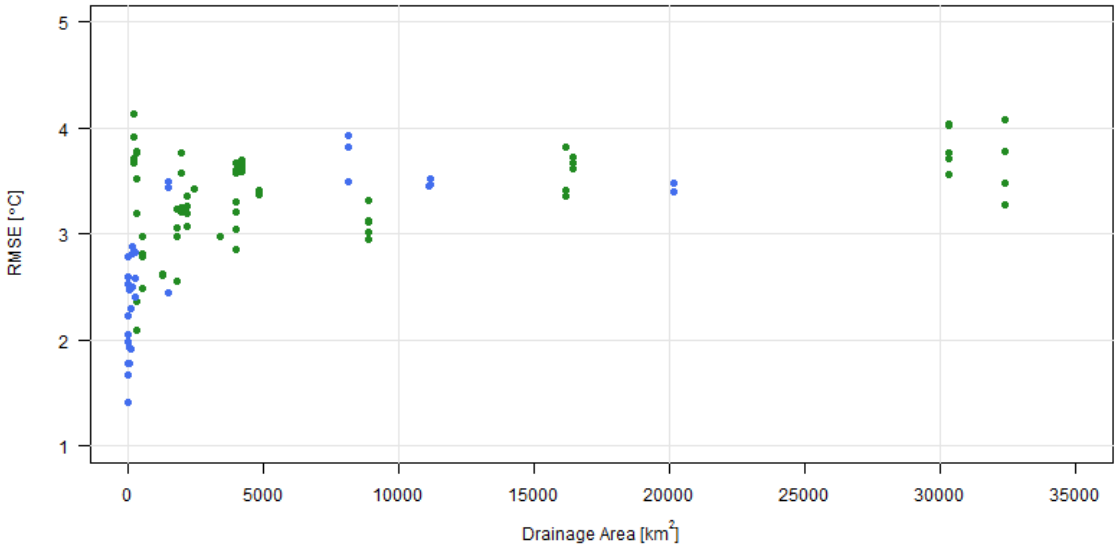

Figure 3.9 Model RMSE versus drainage area size for autumn season datasets (R^2 = 0.240).

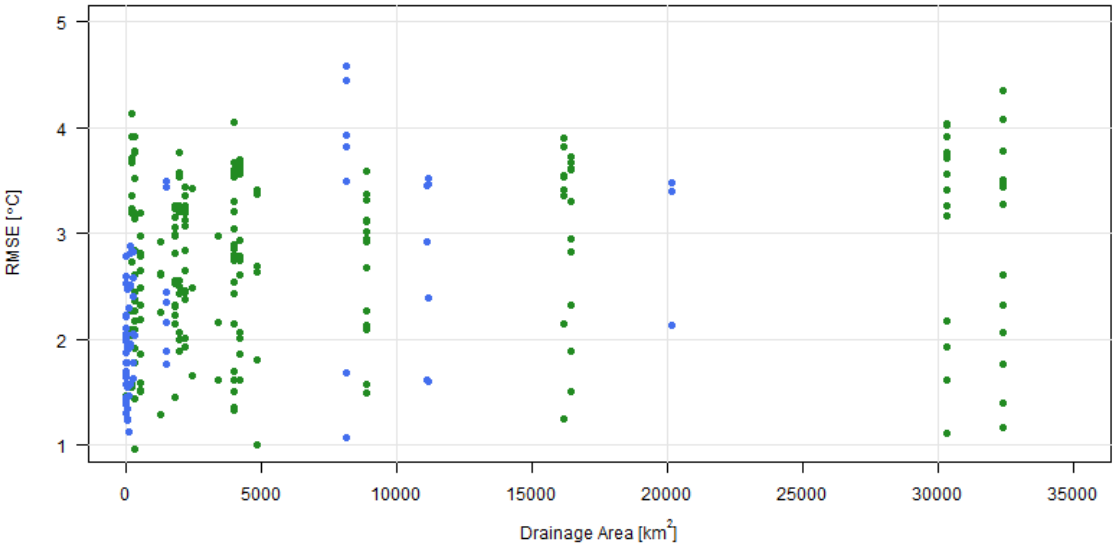

Figure 3.10 Model RMSE versus drainage area size for all seasonal datasets (R^2 = 0.068).

3.3.3 Shift and Drainage Area

The shift hour, as the model parameter that enhances the relationship between air and water temperatures, was found through a systematic search on the least model estimation error criterion for every dataset. The resultant optimum values were used to shift hourly water temperature measurements in-phase with air temperature measurements. The lag in the response of stream temperature to air temperature is most likely caused by the thermal inertia difference between water and air, and is thus dependent on the flow quantity, which directly relates to the drainage area size. While the impact of drainage area size on model estimation error was examined previously, this analysis examines the impact of the drainage area size on the shift parameter. Figure 3.11 shows the scatter plot of the two variables for summer season datasets. From the test statistics, it appears that the drainage area can explain about 16.98% of the variability in shift for summer, and 32.78% and 13.54% for spring and autumn seasons.

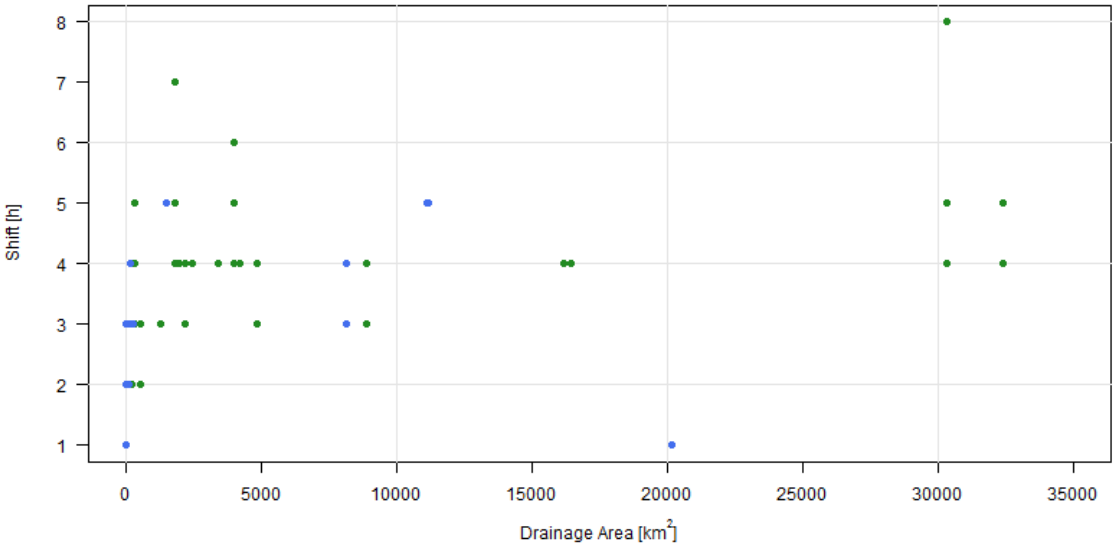

Figure 3.11 Optimized shift hour versus drainage area size for summer season datasets (R^2 = 0.1698).

Notice that despite the small drainage areas, shift values of 6 and 7 hours are present. Since the model selects the optimum shift based on the least model estimation RMSE criterion, even slight improvement in model estimation can alter the shift value. Hence large shifts do not necessarily equate to bad model performance. For example, the summer 2015 dataset for USGS station 05487520 on the Des Moines River near Swan has an optimum shift value of 8 hours, which produces a model RMSE of 1.93 ˚C. The standard deviation of the model RMSEs with all 9 shift values is 0.02 ˚C, with 0 shift hour (original dataset) having the worst performance (1.99 ˚C RMSE). In this case, the high shift value does not associate with bad model performance, nor did it improve the performance drastically.

3.3.4 Model Performance and Distance between Stations

Since the model is built on the relationship between stream and air temperatures, the site-specific models should be developed, ideally, using the temperature measurements taken at the same locations. This would guarantee that the spatial variation in two temperatures would not have any effect on how one relates to the other. However, due to the lack of densely populated stream and air temperature measurement networks on a regular grid, this project, instead, paired USGS and IIHR stream temperature measurement sites with the most adjacent NOAA stations in Iowa. However, the distances in-between the measurement stations vary.

The distance between the temperature measurement stations was studied against the model performance. Figure 3.12 shows the scatter plot of the model RMSE and the distance for all datasets. Figure 3.13 displays only the summer season model RMSE versus distance. There is no observed structure in either case. Test statistics show that the distance between stations explains only about 0.06% variability in the model RMSE for all three seasons' datasets, and about 2% for the summer season. It can be argued that since air temperature does not vary much in space, data measured at stations within 60 kilometers away from each other are valid to use for model development.

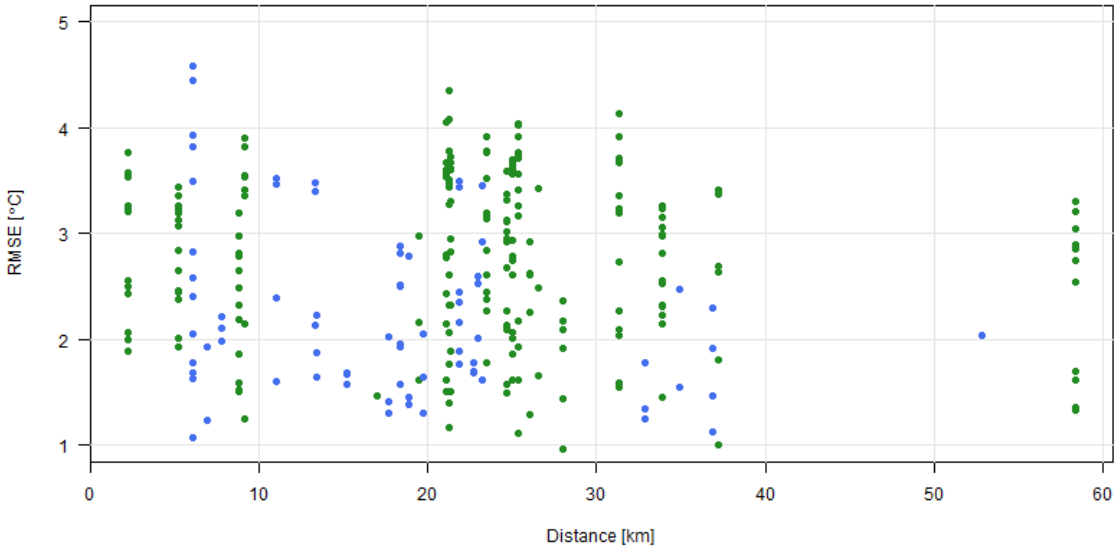

Figure 3.12 Model RMSE versus distance between water and air temperature-measuring stations for all datasets (R^2 = 0.00593).

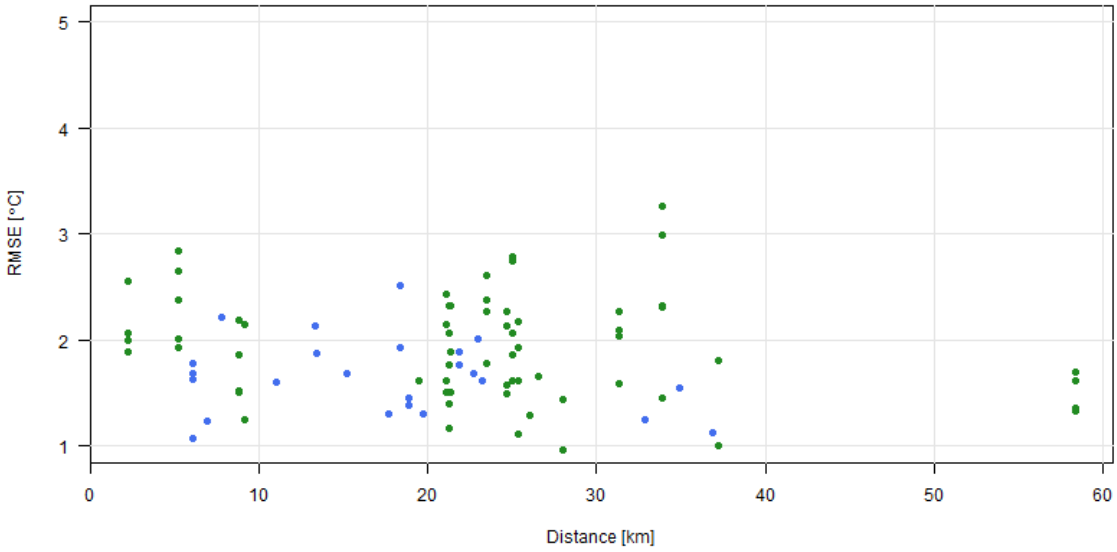

Figure 3.13 Model RMSE versus distance between water and air temperature-measuring stations for summer season datasets (R^2 = 0.0219).

3.4 Conditional Error Analysis

Additive error values present the differences between hourly stream temperature model estimations and the true measurements in degrees Celsius. The hourly additive errors were plotted against both stream temperature and air temperature measurements to study the overall pattern. Error distribution for every 5 °C increase of either temperature was studied for the three seasons separately.

Figures 3.14 and 3.15 both show model performance for the summer season datasets; the first with respect to stream temperature measurements, the latter with respect to air temperature measurements. Figure 3.14 suggests that the model tends to overestimate when stream water temperature is supposed to be low, and underestimate when stream temperature is supposed to be high. The lower and upper tails of the logistic function could be the cause of this strong downward trend. Model estimation approaches two asymptotes that were found, for each dataset, as the minimum or maximum of the measured stream temperature. However, the actual lower and upper limits may in fact be more extreme. Thus the set thresholds could result in poor performance in the tails. It also appears that for every 5 °C increment of stream temperature measurement, the error interquartile range does not vary much and stays less than 4 °C except for the last interval when stream temperature is exceedingly high.

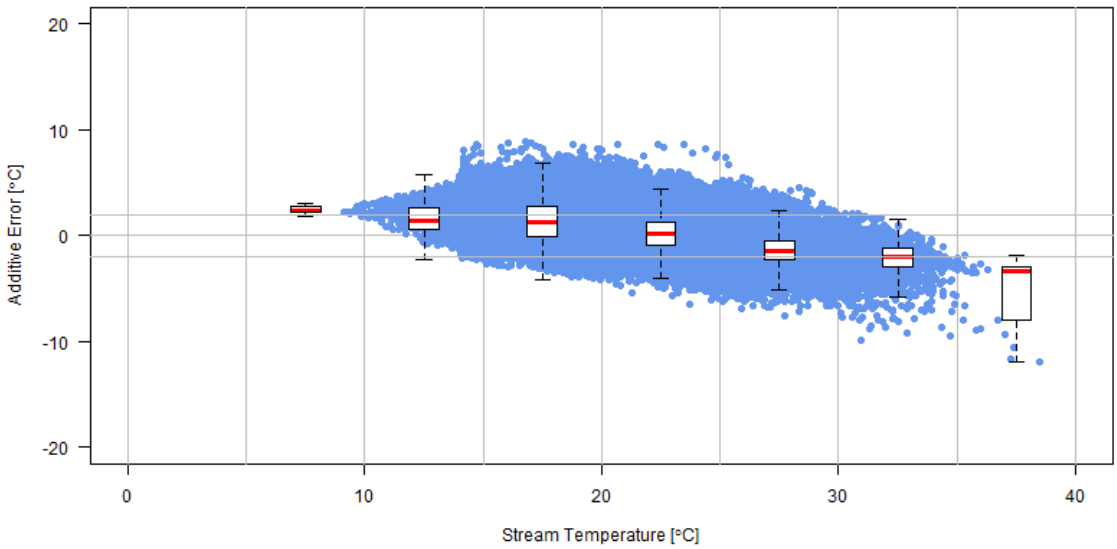

Figure 3.14 Summer stream temperature hourly estimation errors with respect to stream temperature measurements. Extra gridlines indicate ±2 °C band of error requirement.

Similarly, Figure 3.15 shows the error distribution with respect to air temperature, the main model predictor. Unlike the previous plot, this graph suggests that the hourly stream temperature estimation error has consistent performance regardless of the input value of air temperature. The error median stays around 0 °C, which indicates no obvious bias. And for every 5 °C air temperature interval, the interquartile ranges of additive errors do not exceed the span of the ±2 °C requirement.

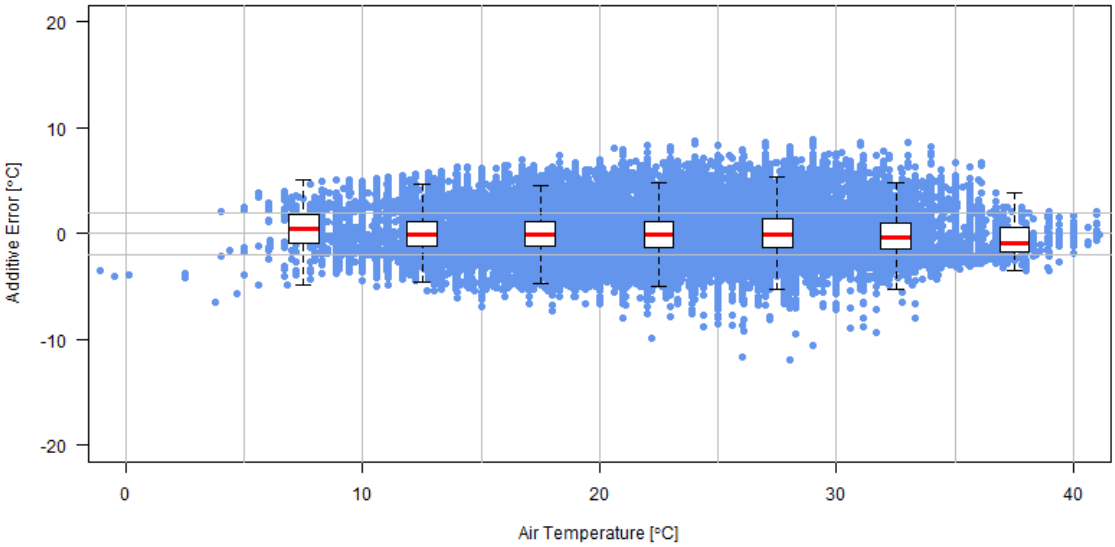

Figure 3.15 Summer stream temperature hourly estimation errors with respect to air temperature measurements.

The estimation error behaviors with respect to changes in stream temperature for spring and autumn seasons are similar to that of the summer season, as shown in Figures 3.16 and 3.17. As the stream temperature approaches 0 °C, the model shows obvious overestimation. This behavior might be associated with freezing and thawing processes under cold weather. The amount of energy absorbed or released during phase change are not considered by the model. However, as evident in Figures 3.18 and 3.19, error distributions with respect to the actual model input show that error medians remain around 0 °C, with interquartile ranges around ±2 °C for spring and autumn.

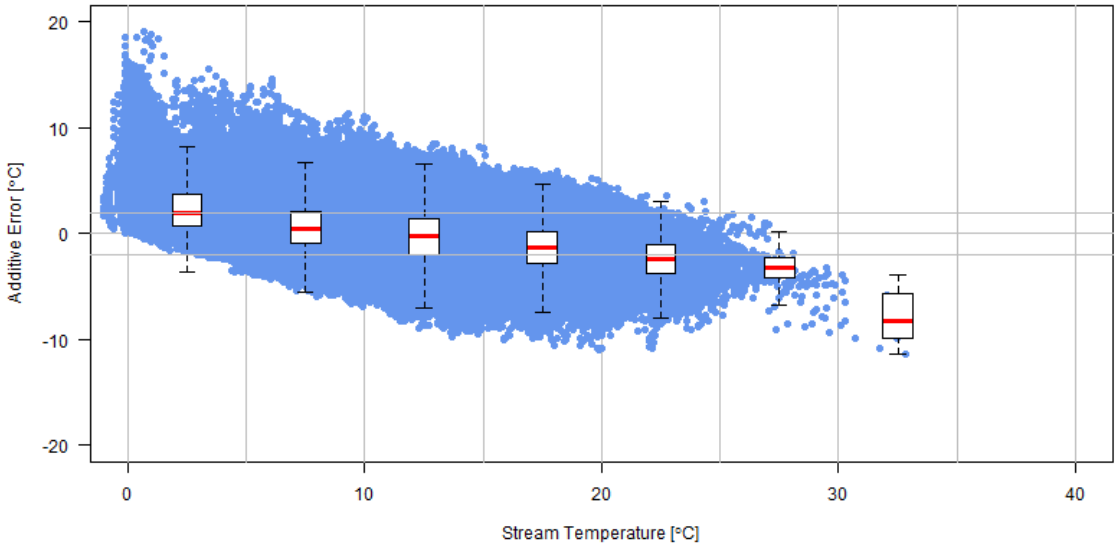

Figure 3.16 Spring stream temperature hourly estimation errors with respect to stream temperature measurements.

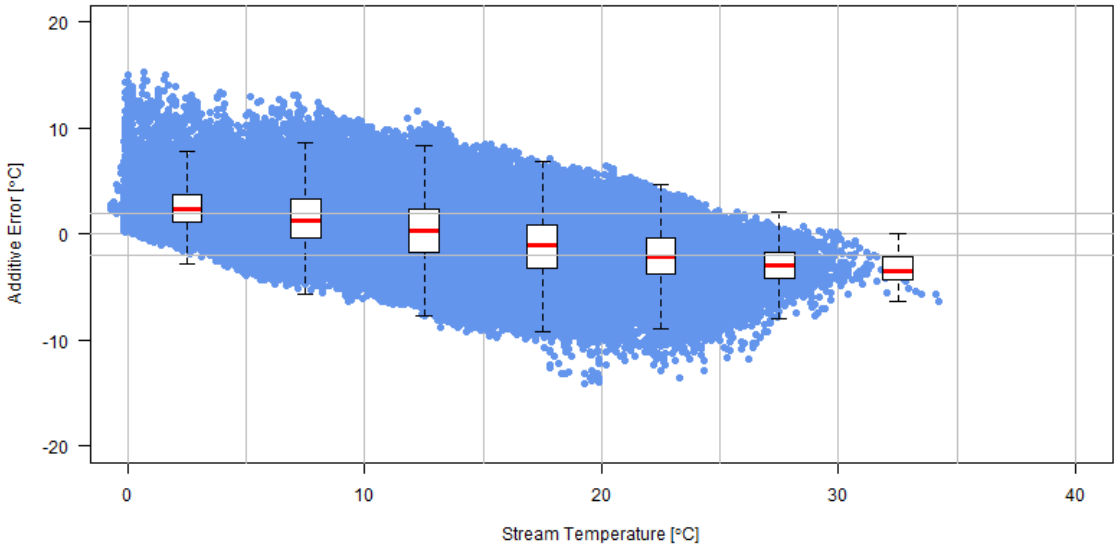

Figure 3.17 Autumn stream temperature hourly estimation errors with respect to stream temperature measurements.

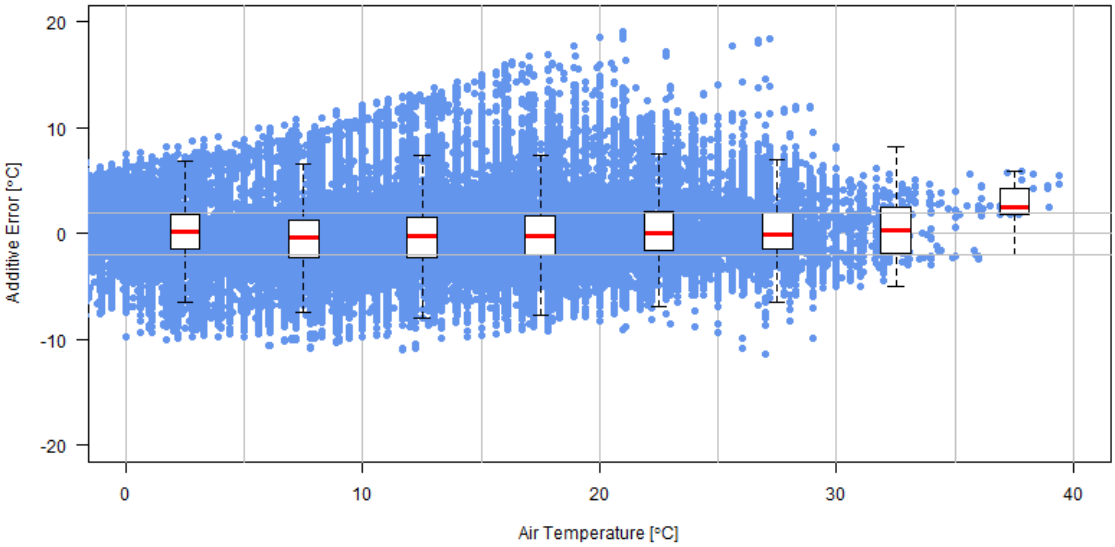

Figure 3.18 Spring stream temperature hourly estimation errors with respect to air temperature measurements.

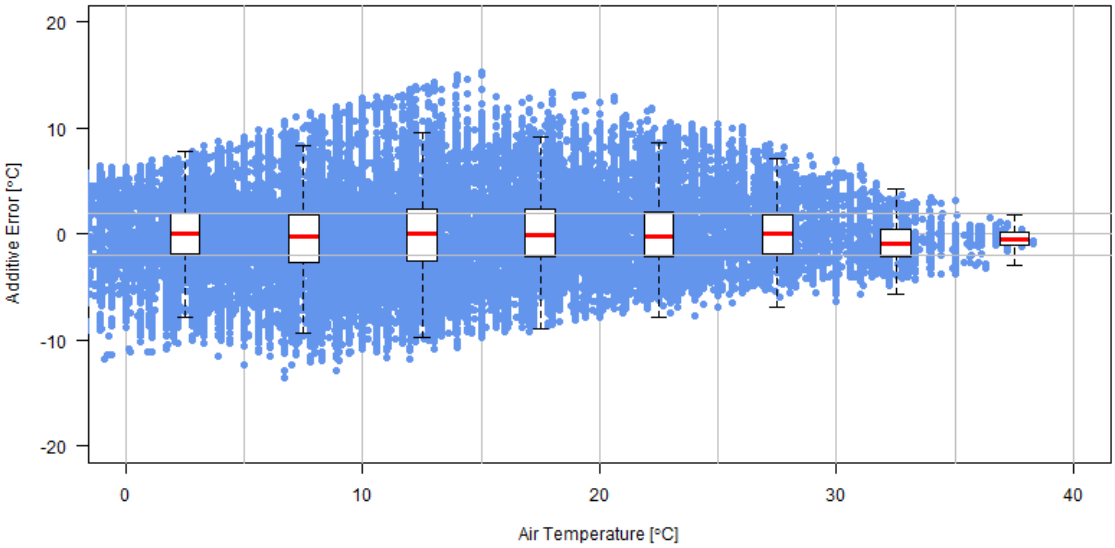

Figure 3.19 Autumn stream temperature hourly estimation errors with respect to air temperature measurements.

From the conditional error analyses, we can see that the additive error in model estimation is inversely related to the actual stream water temperature. However, error

behavior with respect to the main model predictor, air temperature, is of most interest. There is no correlation observed between the two. The error median stays close to 0 ˚C while the first and third quartiles remain around the requirement of ±2 °C. Model performance is the best during summer season, which is ideal as summer is the period of most water quality research interest. Although the model performs relatively poorly under cold conditions, it is not the main priority of this project to predict stream water temperature under cold weather, as the rates of chemical and microbial growth processes are at their minimum. Additive error means for spring, summer and autumn seasons were calculated to be -0.0002 ˚C, 0.07 ˚C, and 0.05 ˚C, respectively. Hence negligible systematic bias was detected for the statistical model.

3.5 Outlier Analysis

Previous analyses focus on studying relationships between different variables that may affect stream water temperature and model performance. A tentative requirement of ±2 °C was set as an acceptable model estimation error. However, outliers exist with poor model performance of over 2.5 °C RMSE. Table 3.1 summarizes the outliers for the summer season datasets. 9 datasets were identified with poor model performance, which consists of 6 stations for 2 model estimation years.

Table 3.1 Outlier datasets for the summer season model estimation.

Water Temperature Site	NOAA Site	Year	DA (km^2)	Distance (km)	Shift (h)	RMSE (˚C)
05482300	SLB	2013	1813	33.9	4	3.26
05482300	SLB	2015	1813	33.9	7	2.99
05481000	EBS	2015	2186	5.27	4	2.85
05482500	PRO	2013	4193	25.1	4	2.78
05482500	PRO	2015	4193	25.1	4	2.75
05481000	EBS	2013	2186	5.27	4	2.66
06604200	SPW	2013	324	23.5	4	2.62
06817000	ICL	2013	1974	2.23	4	2.55
3	CID	2015	158	18.35	3	2.51

The geographical locations of the 6 stations with over 2.5 °C RMSE are shown in Figure 3.20. Although no strong linear relationship exists between model estimation error and drainage area size, the summer stream temperature estimation outliers are for sites within 5000 km^2 of a drainage area. The average RMSEs over the recorded years at each site for spring, summer, and autumn seasons are shown in Figures 3.21, 3.22, and 3.23, respectively. It was also observed that most of the outlier sites are located in the western part of the state.

Compared to large streams, which are more subject to solar radiation and wind, small streams are more subject to riparian vegetation coverage, the impact of which is reduced by bank to bank farming practices. Streambed and groundwater heat fluxes can also become significant portions of the total heat flux in small streams, especially during spring and autumn seasons. The western Iowa region is largely composed of farm lands, and has relatively fine river bed materials, such as sandy clay and loam, which are good heat conduction mediums. Due to tile drainage practices, the groundwater inflows merge into the streams with different temperatures. Hence the small steams in western Iowa are

more exposed to solar radiation, streambed heat flux, and groundwater heat flux that the model fails to account for, leading to relatively poor performance on such streams.

Comparatively, the north-eastern Iowa region has mostly hilly terrain and relatively coarse river bed materials, along with high riparian coverage. These factors prohibit the stream temperature from fluctuating as dramatically as it would under the same meteorological conditions at a site located in the western region of Iowa. The Turkey river site serves as an example of good model performance in north-eastern Iowa.

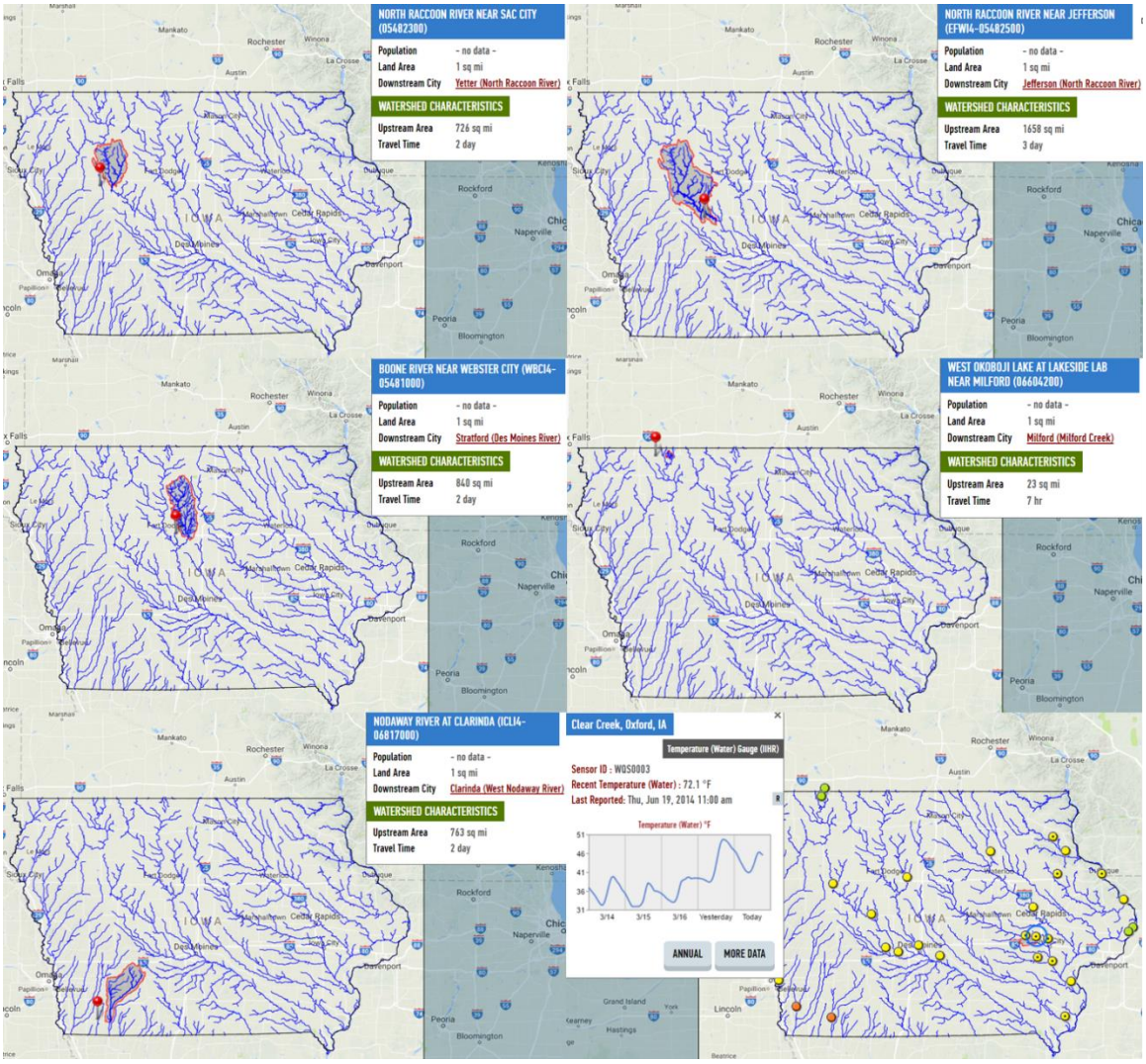

Figure 3.20 Geographical locations of summer outlier stations with over 2.5 °C RMSE.

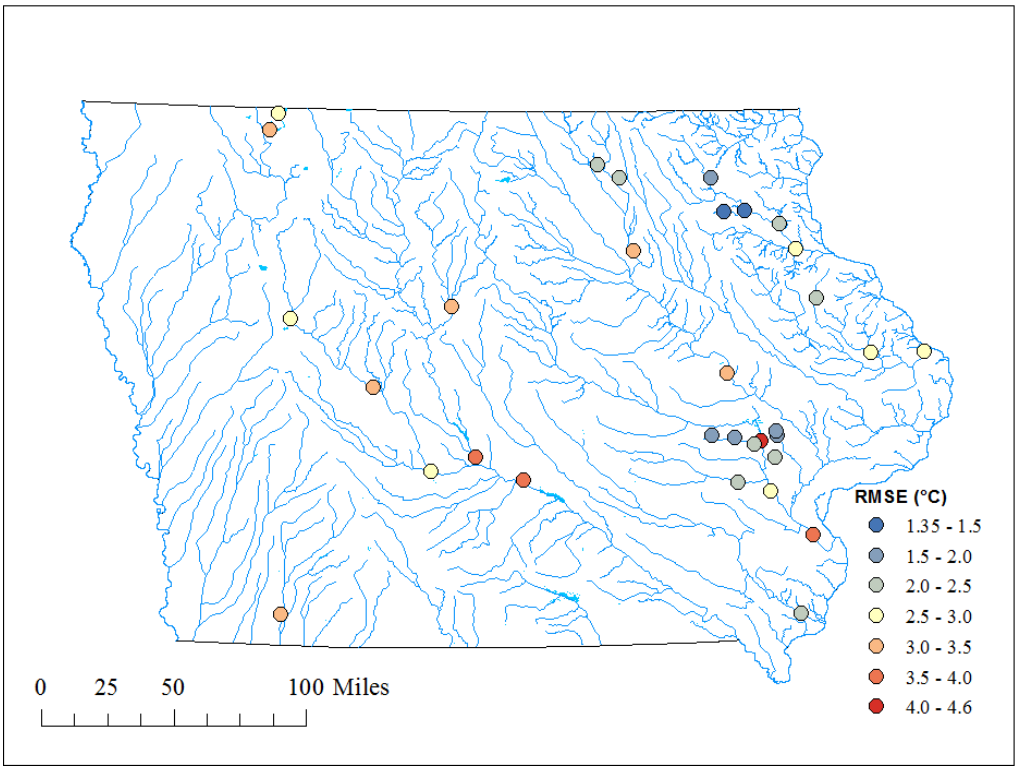

Figure 3.21 Spatial representation of spring average RMSEs over the recorded years.

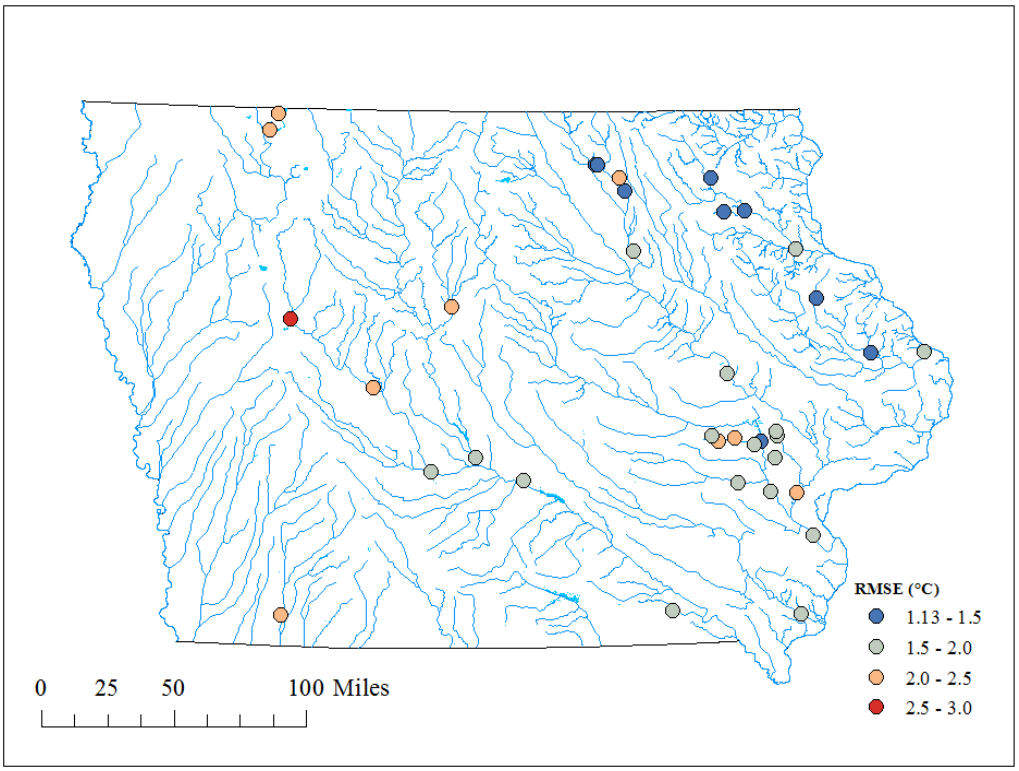

Figure 3.22 Spatial representation of summer average RMSEs over the recorded years.

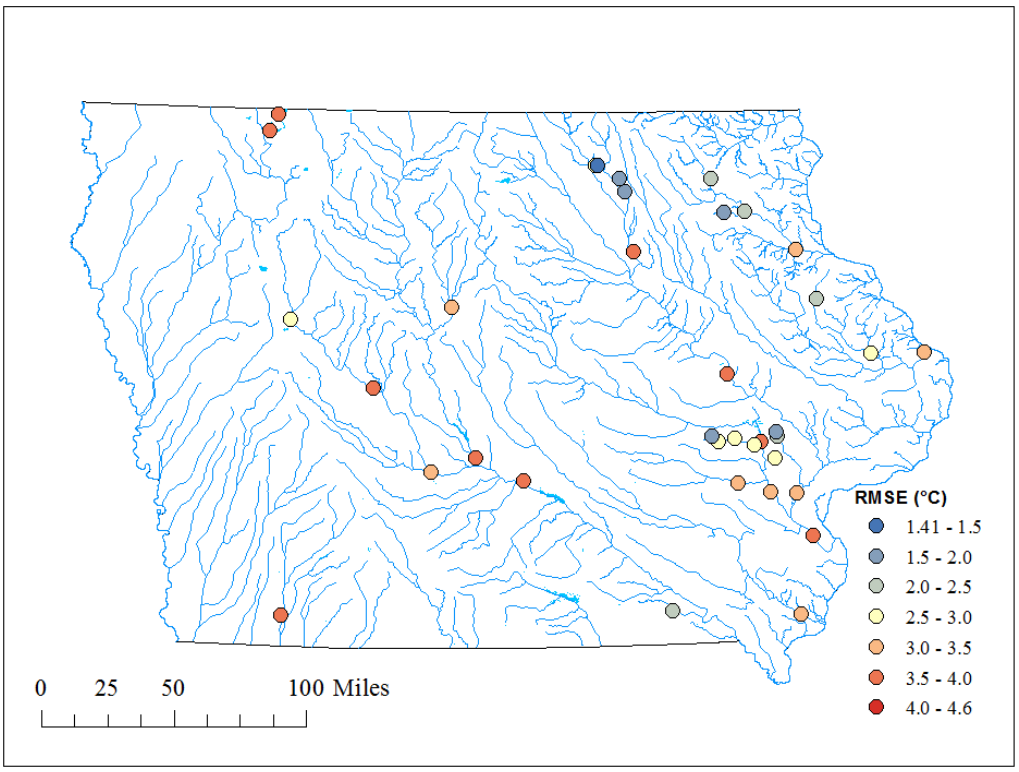

Figure 3.23 Spatial representation of autumn average RMSEs over the recorded years.

Table 3.1 indicates that the years in which the summer outliers occurred were either 2013 or 2015. The annual time series plot of stream and air temperature measurements, as well as the discharge amount at USGS station 05482300 on North Raccoon River near Sac City (hereafter referred to as the North Raccoon River site) are shown in Figure 3.24. It is apparent that 2013 had a wet spring season leading into dry summer and autumn seasons. The relationship between stream and air temperatures is different for the precipitation high and low precipitation periods. As observed in Figure 3.25, the stream temperature before July, which is the end of the high precipitation period, matched air temperature fluctuations with low moving averages and small oscillation amplitudes. The stream temperature after August remained on the higher part of the oscillation of air temperature fluctuations, with relatively big amplitudes.

Although it was found previously that no apparent correlation exists between model performance and normalized discharge, the hydrologic regime seems to have an overall impact on the stream-air temperature relationship. Stream temperature reacts more distinctly to changes in meteorological conditions under a precipitation-scarce period, and does not cool down to match the lower values of the air temperature oscillation. It is worth mentioning that the model RMSEs are 2.52 °C and 2.97 °C for spring and autumn 2013 at this site. Comparatively, the model estimation error for the summer of 2014 at the North Raccoon site is only 1.45 °C. As shown in the annual time series plot in Figure 3.26, 2014 was a hydrologically normal year. The high discharge amount in summer balanced the high fluctuations of stream temperature under hot weather conditions.

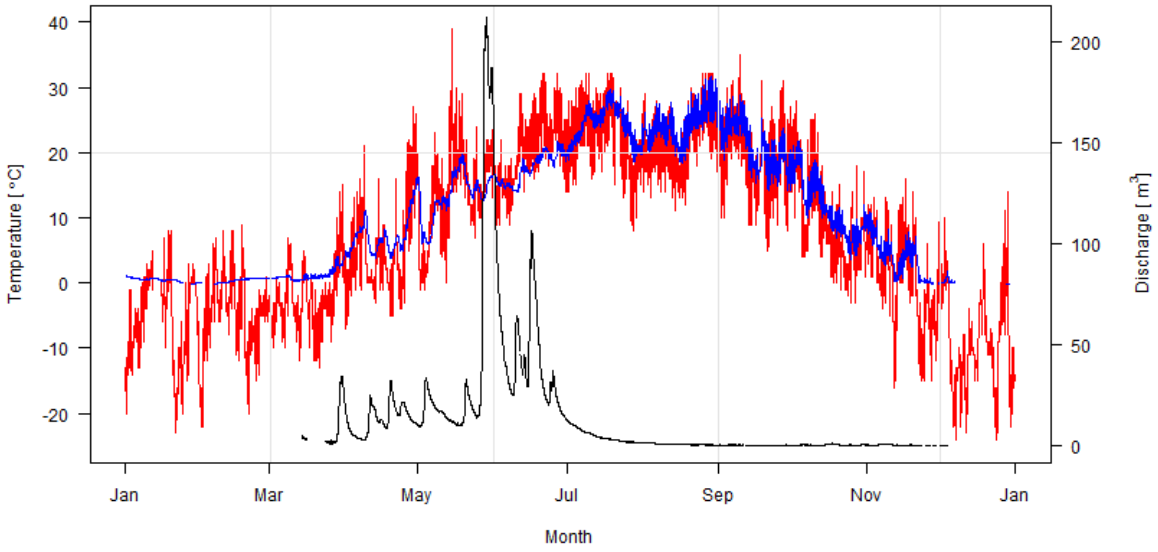

Figure 3.24 2013 annual hourly stream and air temperatures and discharge time series at North Raccoon site.

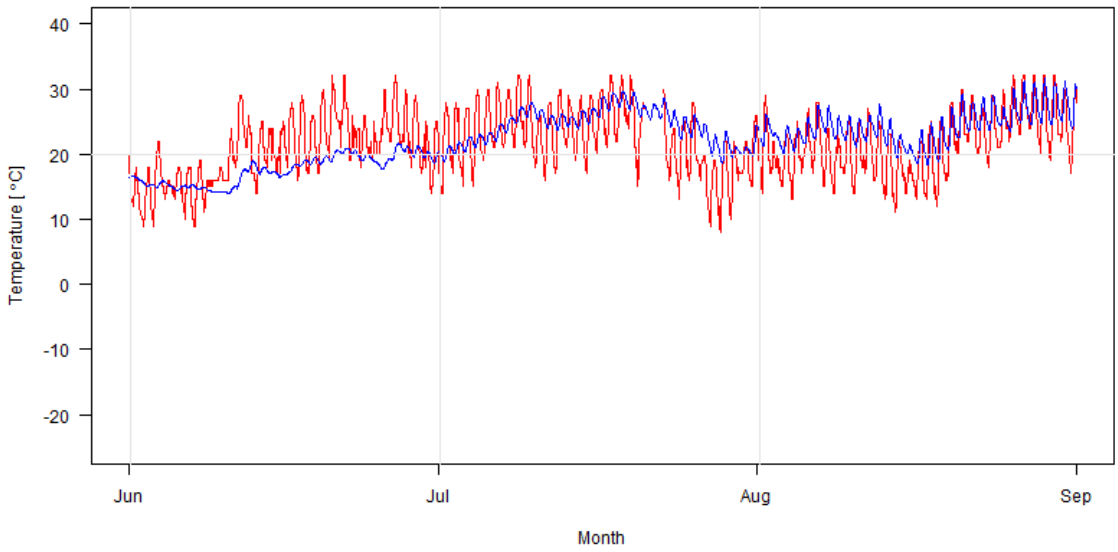

Figure 3.25 2013 summer hourly stream and air temperatures and discharge time series at North Raccoon site.

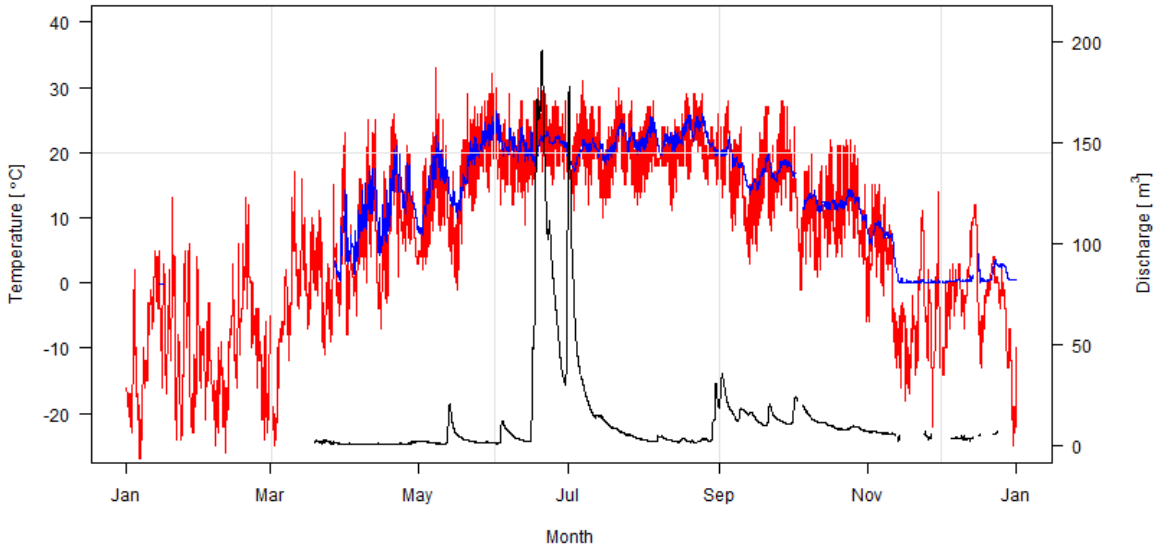

Figure 3.26 2014 annual hourly stream and air temperatures and discharge time series at North Raccoon site.

The regression model assumes normal hydrologic regime, hence does not capture the air-water relation under different regimes. Figure 3.27 illustrates the comparison

between the simulated and observed stream temperature for the summer of 2013 at the North Raccoon site. It appears that instead of considering the steam temperature variations due to hydrologic regime alterations, the model assumes that the same relation exists between air and water temperatures throughout the period. Hence the estimated values fail to match the dampened amplitudes and the shifted moving maximums and minimums of the observed stream temperature.

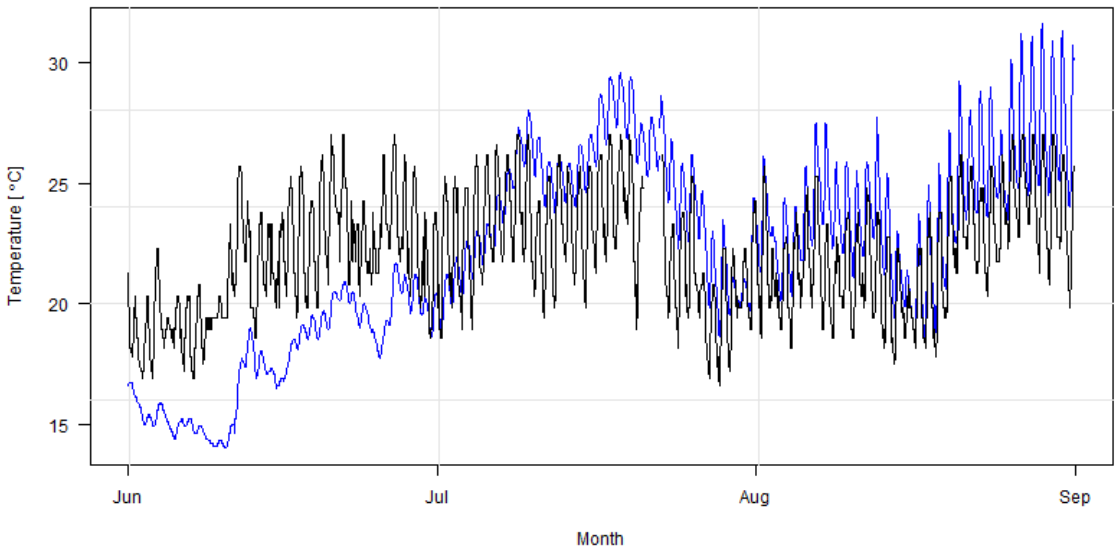

Figure 3.27 Summer 2013 stream temperature hourly observations and estimations at the North Raccoon site. Blue: hourly observed stream temperature. Black: hourly estimated stream temperature.

3.6 Reservoirs

As discussed previously, lakes and reservoirs are not treated differently from a normal stream reach in the statistical model. There are three major reservoirs in the state of Iowa: Saylorville Lake Reservoir and Lake Red Rock Reservoir, both located on the Des Moines River, and Coralville Lake Reservoir on the Iowa River. USGS Site 05482000 on the Des Moines River at 2nd Ave is located downstream of Saylorville Lake

Reservoir, and upstream of Lake Red Rock Reservoir (Figure 3.28). Despite being located between two reservoirs, the site exhibits good model estimation performance of 1.25 °C RMSE for the summer of 2014. Additionally, USGS Site 05487520 on the Des Moines River near Swan, which is located downstream from the previous site (Figure 3.29), also shows exceptionally good performance of 1.12 °C RMSE for the summer of 2014.

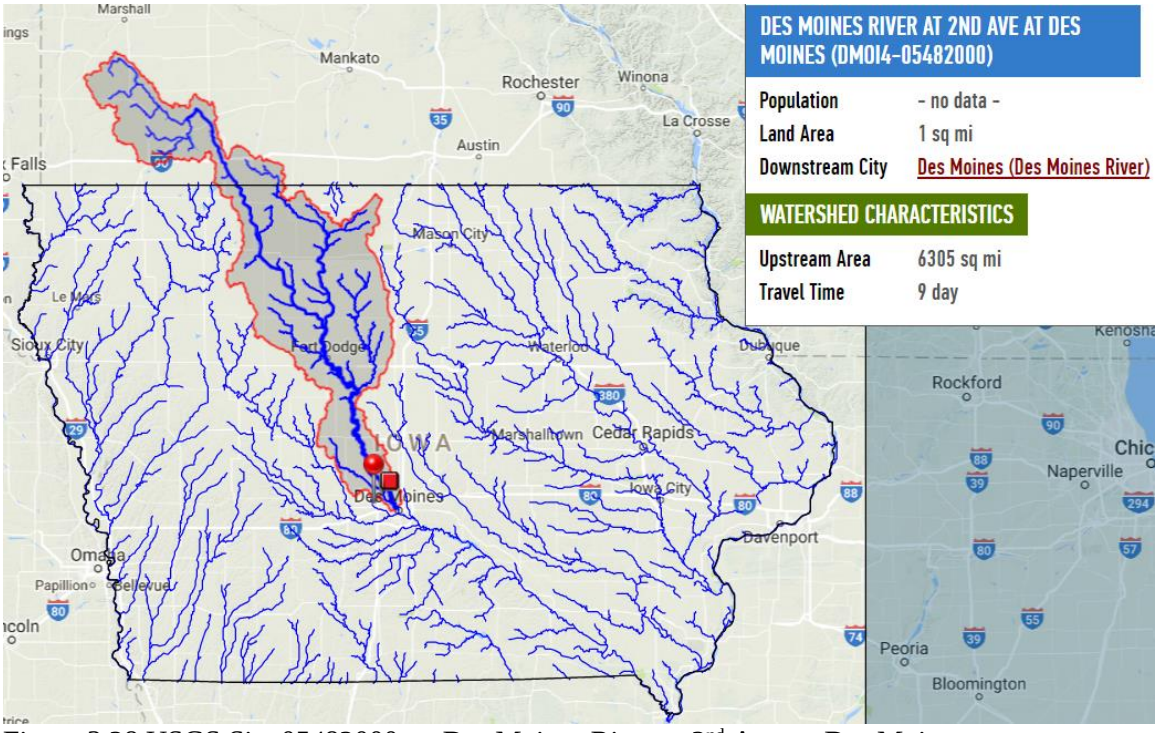

Figure 3.28 USGS Site 05482000 on Des Moines River at 2nd Ave. at Des Moines.

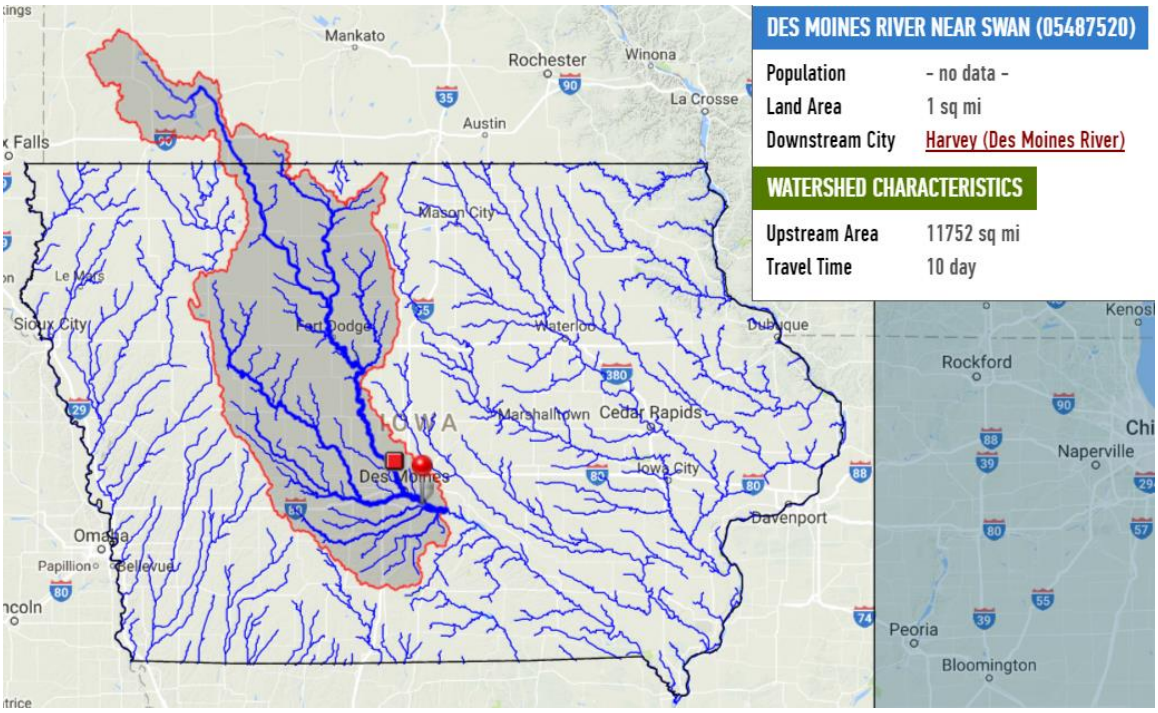

Figure 3.29 USGS Site 05487520 on Des Moines River Near Swan.

The two main factors that could largely affect the stream-air temperature relationship downstream from reservoirs and lakes are the water temperature stratification effect and the considerable amount of water released. Since no explanatory relationship was found between discharge and model performance, the amount of water released should not be a strongly influential factor for the water temperature downstream. The flood-control reservoirs in Iowa have relatively small magnitudes, hence the temperature stratification effect could be insignificant enough. Therefore, the decision to not treat reservoirs and lakes as separate entities in the model was justified.

3.7 Energy Budget

As per the outlier analyses, the solar radiation and streambed and groundwater heat fluxes not considered by the statistical model contribute to causing uncertainty in

model performance. These heat fluxes are not directly related to air temperature, and thus do not contribute to the model prediction. Research has shown that while comparing energy components, shortwave (solar) radiation is the most dominant of the total energy flux (Caissie, 2006), and can be especially significant for agricultural watersheds (Younus et al., 2000). To illustrate this, I calculated the percentage of solar radiation in total energy flux for August 1st, 2016 at USGS Site 06817000 on the Nodaway River at Clarinda.

From Equations (7) and (8), the convective heat flux equation can be reduced to:

$$Q_H = 0.11123 * Q_E \left[\frac{(T_s - T_a)}{(0.1608 \exp(\frac{17.27 T_s}{237.3 + T_s}) - e_a)} \right] \quad (22)$$

Values of shortwave radiation, longwave radiation, evaporative heat flux, and air temperature were acquired from the IFC evapotranspiration calculation database. The atmospheric vapor pressure was calculated as

$$e_a = 0.6108 \exp(\frac{17.27 T_a}{T_a + 237.3}) \quad (23)$$

The solar radiation percentage in the net radiation was calculated to be about 63% on average in the hours with available solar radiation, and standard deviation was about 22%. The percentage in the total energy flux was about 26% with a standard deviation of 14%. Hence a considerable part of the energy flux that influences stream temperature is absent from the statistical model. Including it in a more complete model should reduce the prediction error.

3.8 Chapter Summary

Through explanatory analyses that compare model performance with different variables, it was found that the discharge amount, drainage area size and distance between temperature stations do not have direct influence on model performance. However, drainage area size can explain some variability in the shift parameter. The hourly stream temperature estimation errors do not vary much with respect to changes in the model input of air temperature. However, the model performs poorly in capturing the upper and lower tails of stream temperature, possibly due to the set thresholds of temperature minimum and maximum.

Heterogeneity exists in model performance, both geographically and hydrologically. The model performs less well on small streams in western Iowa, possibly due to the low riparian coverage, conductive bed material, and tile drainage inflows. Different hydrologic regimes can also alter the stream-air temperature relationship, creating inconsistency in model performance. Reservoirs and lakes do not introduce extra, unexplained behavior in model performance, and are considered as normal stream reaches by the model.

To quantify the percentage of energy flux unaccounted-for by the model that influences stream temperature, the solar radiation percentage in total energy flux was calculated for a summer day at a western Iowa site. The results indicate that the statistical model does not consider a significant portion of the energy flux, introducing temperature patterns that the model fails to capture.

CHAPTER 4 OPERATIONAL IMPLEMENTATION & VISUALIZATION

4.1 Introduction

The site-specific model developed and evaluated previously was integrated into a state-wide product that can generate real-time hourly stream temperature estimations for both current and forecasted conditions. The season-specific model parameters were interpolated onto the cropped HRRR 3-kilometer Lambert Conformal grid for Iowa to match with the air temperature input. The results are then transferred onto river networks through grid to link association. The river network derived from a USGS 90 m DEM consists of 419,157 channel links in the state of Iowa, of which 3,812 are for streams of 4^{th} order and up. The real-time stream temperature estimations are visualized on the Beta version of the Iowa Water Quality Information Systems, Beta version (IWQIS Beta) portal.

4.2 State-Wide Grid Parameterization

4.2.1 Seasonal Site-Specific Parameters

The summer season logistic regression parameter distributions appear in Figure 4.1. The estimated maximum (α) and minimum (μ) stream temperatures, as well as the air temperature at the inflection point (β), all have interquartile ranges of less than 5 ˚C. The slope of the logistic function at the inflection point (γ) has an interquartile range of less than 0.05. As per the conditional error analyses, the over- and under-estimation at the lower and upper tails of stream temperature might be caused by minimum and maximum

thresholds set by the measured data of the estimation period. Hence the stream temperature thresholds, α and μ, will be the historical high and low values recorded at each site over the years for each specified season.

The density distributions of the regression parameters for summer season datasets also suggest that the parameters follow a normal distribution. The β and γ values are associated with the inflection point of the logistic function. Hence the β and γ values will be the averages of the estimated values at each site over the years for each specified season.

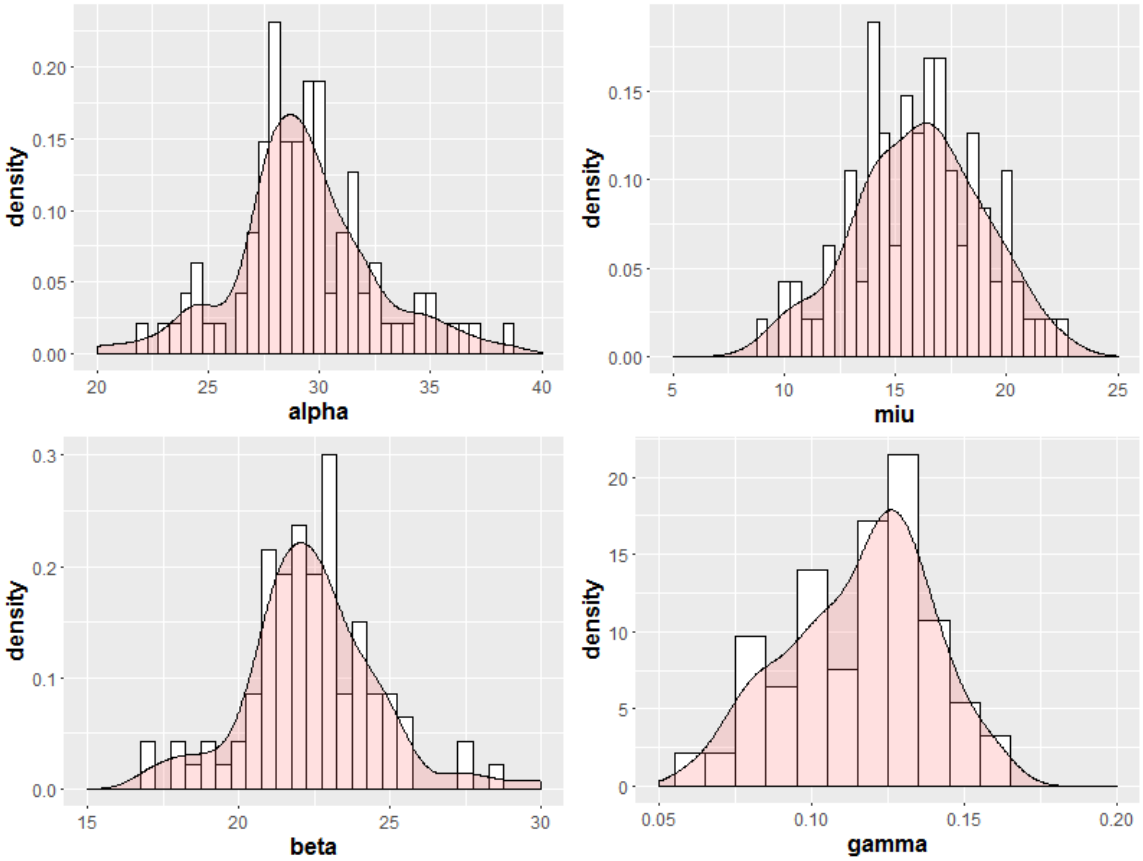

Figure 4.1 Probability density distributions of the logistic parameters for summer season datasets (α IQR = 3.25 ˚C; μ IQR = 4.15 ˚C; β IQR = 2.36 ˚C; γ IQR =0.031).

The shift parameter distribution appears in Figure 4.2. The most frequent shift values are 3, 4 and 5 hours. Note that high shift values do not imply poor model

performance. Hence the shift value at each site could be set as the seasonal average over data record years. However, since an explanatory relationship exists between shift and the drainage area size, shift can also be determined through a simple linear function using drainage area as the predictor. This linear function can be developed empirically for each season. Both methods were used alternatively to investigate which one offers optimum model performance.

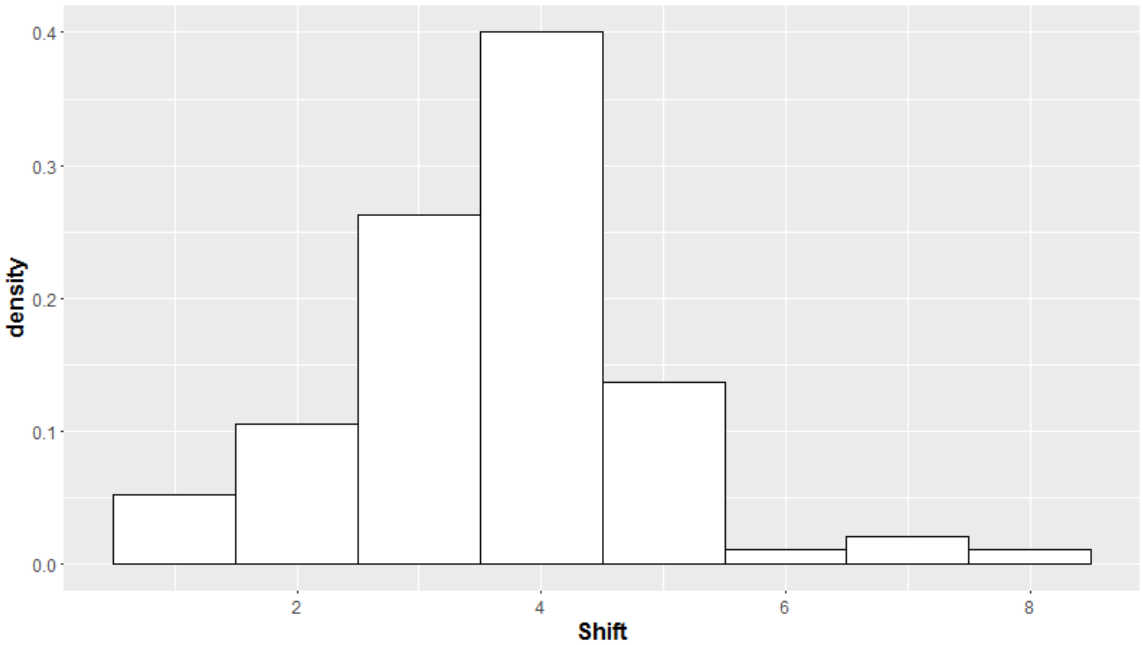

Figure 4.2 Probability density plot of the shift parameter (IQR = 1 hour).

4.2.3 2016 On-Site Model Evaluation

In order to evaluate the statistical model performance on stream temperature prediction, I performed on-site model evaluation using 2016 measurement data and seasonal site-specific parameter values estimated from datasets prior to 2016. I conducted model evaluation using two different methods for the shift parameter estimation: one took the seasonal site-specific average of the historical fitted values, and the other used

drainage area as the independent variable in empirically fitted linear functions. A summary of the evaluation results appears in Table 4.1. As observed, the average seasonal RMSEs across the sites do not exceed 3 °C, with standard deviations of within 1 °C, regardless of the shift estimation approach. Furthermore a simple average of the fitted shift parameter values from the previous years outperforms the linear function shift estimation approach by about 0.038, 0.014, and -0.012 °C for spring, summer, and autumn, respectively. Because the differences in estimation error are negligible, the averaging shift method is the better and simpler approach for model implementation. Tables A-5, A-6, A-7 in the Appendix document the model parameter values for each season and site. The model estimation RMSEs for spring, summer, and autumn of 2016 at every site appear in Table A-8 in the Appendix.

Figures 4.3, 4.4, and 4.5 show the spatial representation of model estimation error for the year of 2016, using the averaged shift parameter values. Northeastern Iowa generally appears to perform better than the rest of the state. The summer season model performance is the best of all three seasons, which generates an average RMSE of 1.77 °C, below the 2 °C standard.

Table 4.1 2016 on-site model evaluation results with different shift estimation methods.

Season	Number of Sites	Average RMSE (°C)		Standard Deviation of RMSE (°C)	
		Averaged Shift	Linear Model Estimated Shift	Averaged Shift	Linear Model Estimated Shift
Spring	27	2.95	2.99	0.985	0.955
Summer	27	1.77	1.79	0.497	0.523
Autumn	24	3	2.99	0.926	0.964

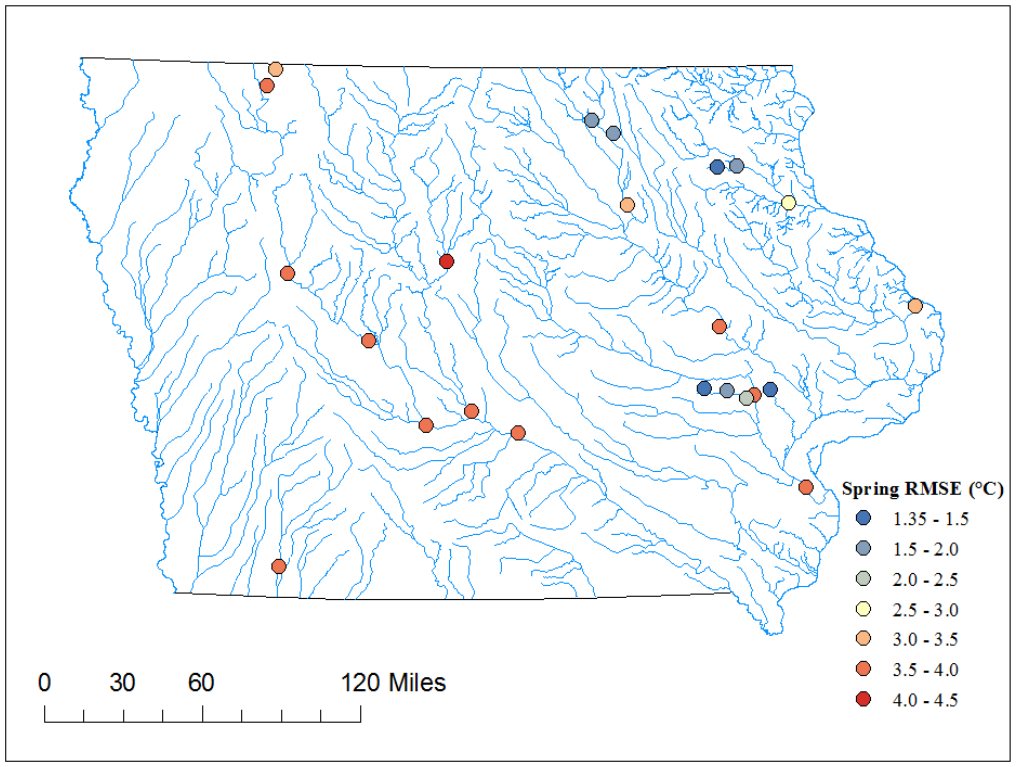

Figure 4.3 Spatial representation of 2016 spring on-site model evaluation RMSE. (Average RMSE = 2.95 °C; standard deviation of RMSE = 0.99 °C).

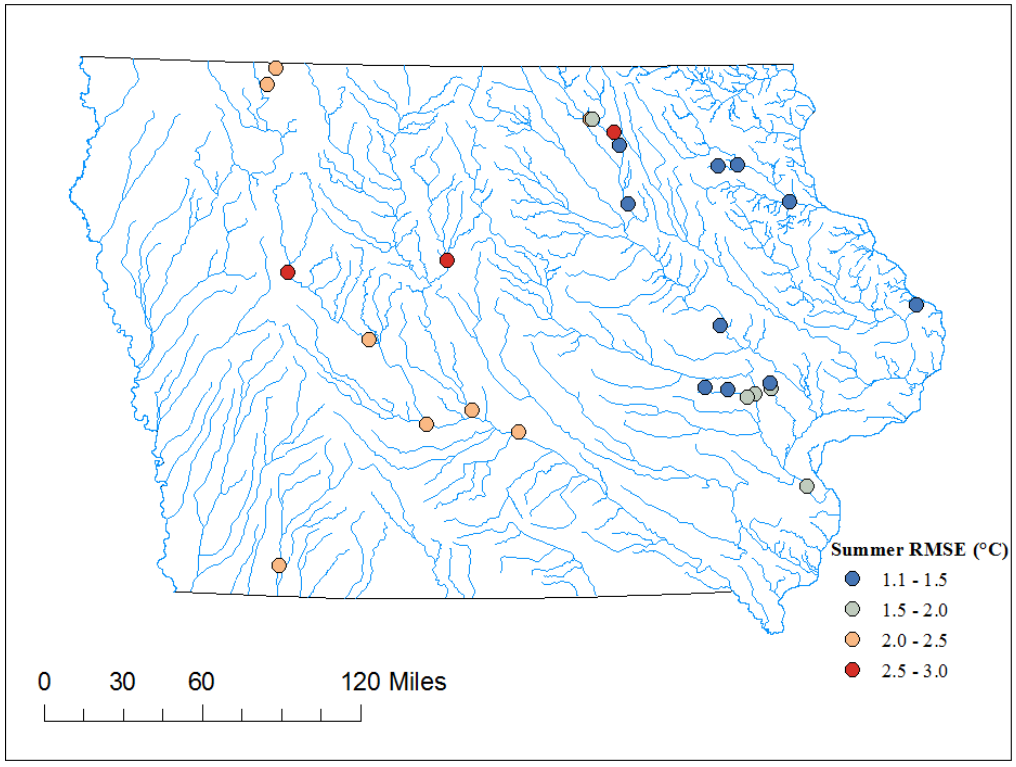

Figure 4.4 Spatial representation of 2016 summer on-site model evaluation RMSE. (Average RMSE = 1.77 °C; standard deviation of RMSE = 0.50 °C).

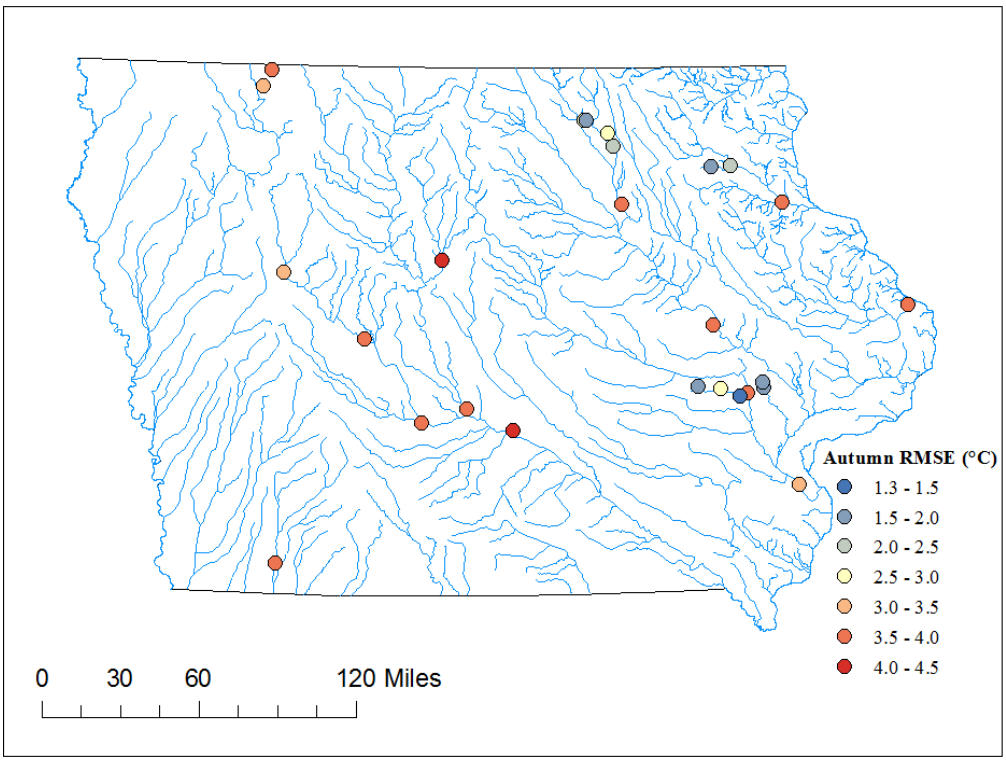

Figure 4.5 Spatial representation of 2016 autumn on-site model evaluation RMSE. (Average RMSE = 3.00 °C; standard deviation of RMSE = 0.93 °C).

4.2.2 State-Wide Parameter Integration

The Inverse Distance Weighting (IDW) method was used to interpolate the seasonal site-specific parameter values onto the HRRR product grid to achieve state-wide model implementation. Equation (24) shows the IDW method formulation,

$$\lambda_i = \frac{(1/x_i)^2}{\sum_{i=1}^{n}(1/x_i)^2} \tag{24}$$

where λ_i is the weighting factor for the i-th site, x_i is the parameter value at the i-th site, and n is the number of measurement-available sites.

The Lambert Conformal conic projection 3-kilometer resolution HRRR Grib file was cropped to the Iowa boundary. To achieve gird parameterization for every pixel in

the state, IDW spatial analyst tool in ESRI ArcGIS was utilized, generating state-wide rasters for each parameter and season. Figure 4.6 shows the spring season α value raster. The parameter field exhibits some rapid variations in space in the eastern part of the state, where the stream temperature measurement network is more populated. Comparatively, the less well-sampled regions, generally the western part of the state, exhibit more gradual variations in parameter values.

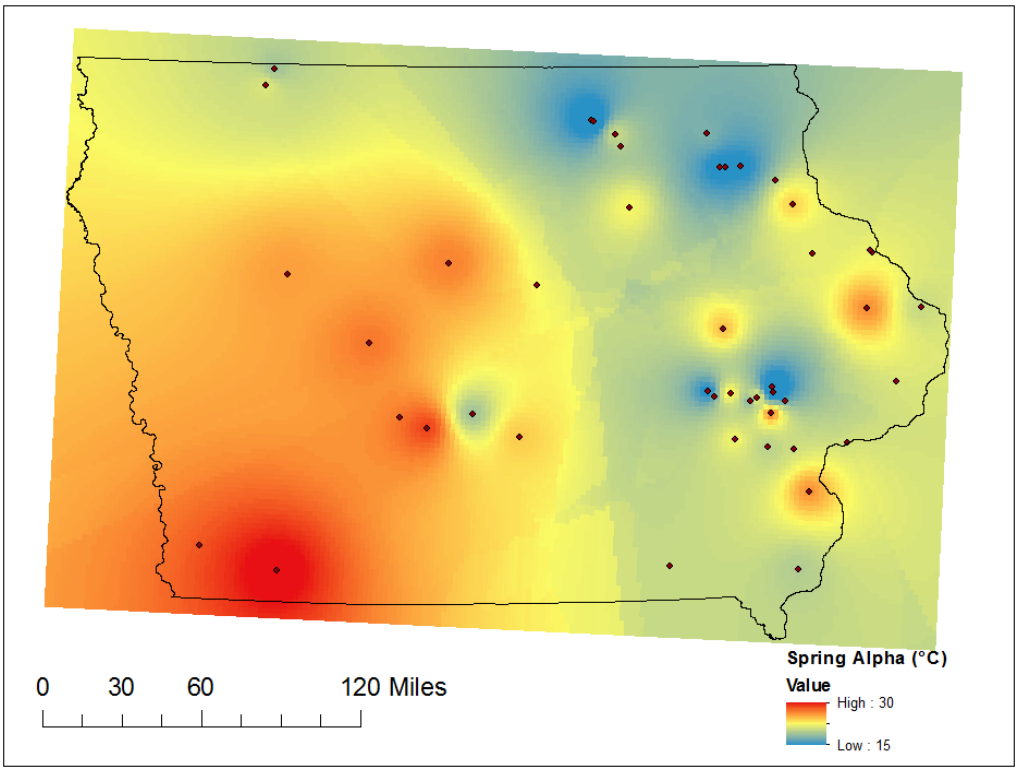

Figure 4.6 State-wide spring alpha (α) parameter value raster.

4.4 State-Wide Stream Temperature Computation

Hourly data for the model's explanatory variable, air temperature, is available from the High-Resolution Rapid Refresh (HRRR) product generated by the NOAA National Centers for Environmental Prediction (NCEP). According to NOAA, the HRRR is a "real-time 3-km resolution, hourly updated, cloud-resolving, convection-allowing

atmospheric model, initialized by 3-km grids with 3-km radar assimilation" (NOAA, 2017b). The product is available for the entire United States, and provides current as well as forecasted air temperature estimations for 18 hours in advance. Thus the statistical stream temperature model can be computed on the same 3-km HRRR grid for the state of Iowa.

Figure 4.7 shows the HRRR air temperature estimation for Iowa at the 4 pm of March 30th, 2017. As expected, the northern part of the state is generally warmer than the east. Anomalies exist with certain cells having relatively higher air temperatures than the surrounding cells. However, when overlaid with the river network, as shown in Figure 4.8, the anomalies only appear to occur over large water bodies, including large rivers, lakes, and reservoirs. Such behavior is especially apparent on the Mississippi River.

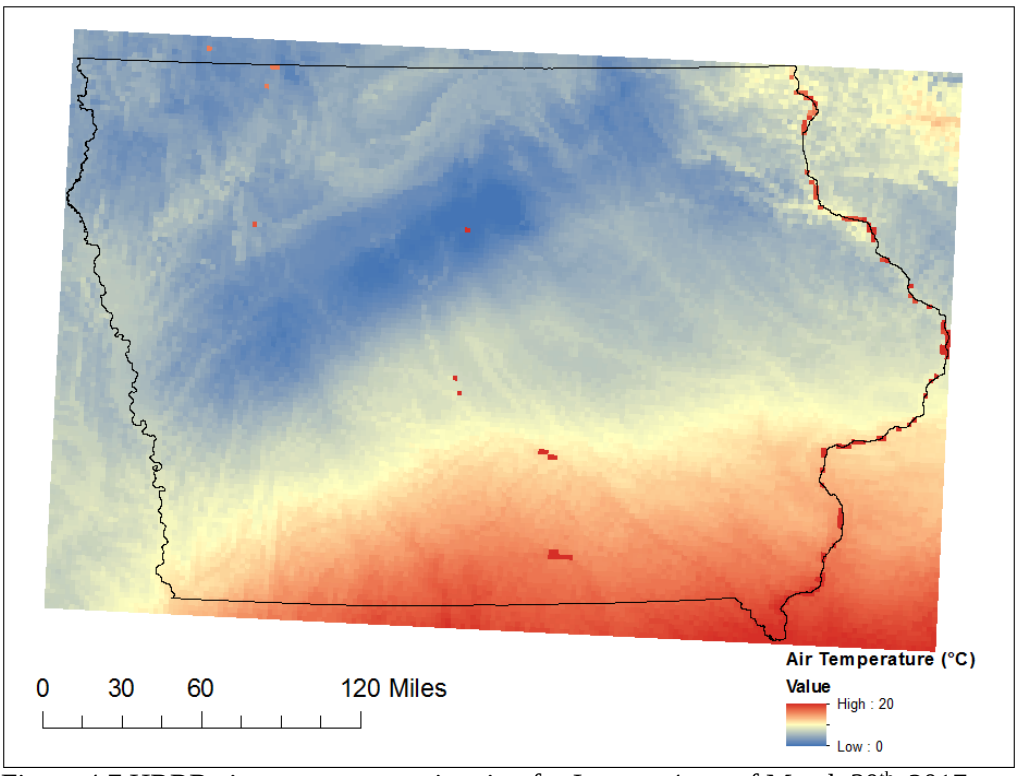

Figure 4.7 HRRR air temperature estimation for Iowa at 4 pm of March 30th, 2017.

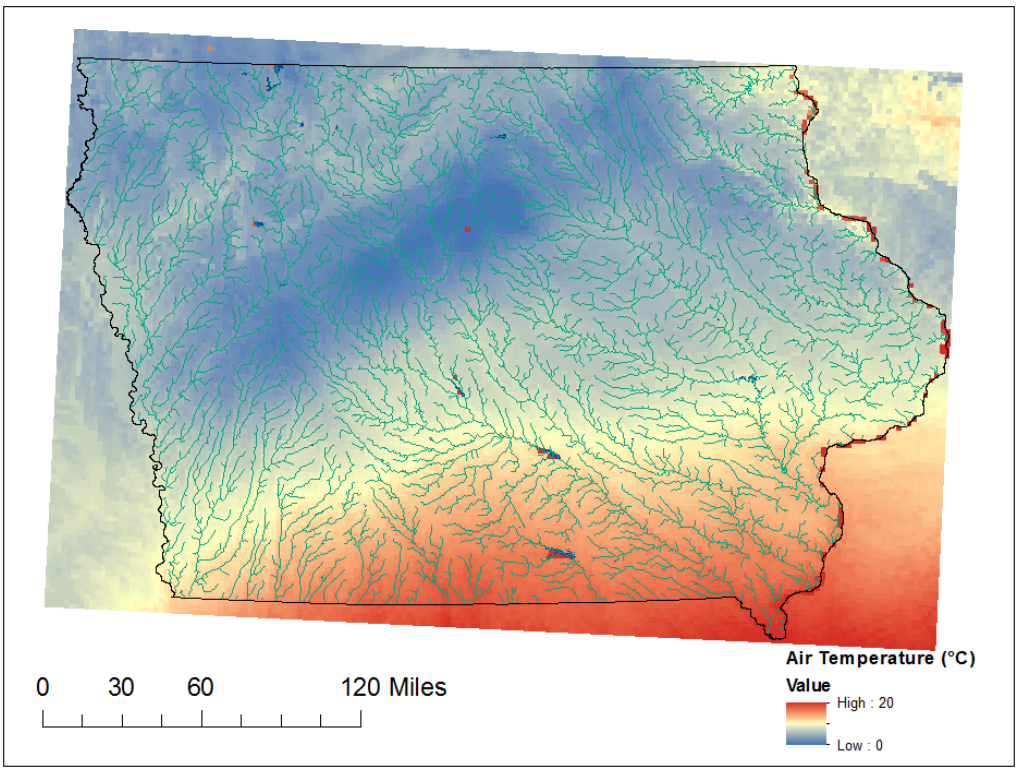

Figure 4.8 HRRR air temperature estimation for Iowa at 4 pm of March 30th, 2017, overlaid with the river network.

State-wide stream temperature estimation was computed for 4 pm of March 30th, 2017 on the HRRR grid. Hourly HRRR air temperature estimations from 11 am March 29th to 4 pm March 30th, 2017 were used, to account for the time lag component. The computed results kept the overall patterns in the explanatory variable as well as the interpolated spring season parameter rasters. While the spatial variations in the gridded stream temperature estimation and the fact that it is available on every 3-km pixel in the state may seem unrealistic, it is helpful to keep in mind that the statistical model does not account for the propagation of water. Thus the estimated results assemble the spatial patterns in both the model explanatory variable and the regression parameters. The gridded results were later transformed onto river networks, which then possess physical meaning.

4.5 HRRR Grid to Hillslope-Link

The IFC system uses a river network derived from a 90-meter USGS Digital Elevation Model (DEM). The network consists of about 620,000 links, of which 419,157 are inside the state of Iowa. The links have lengths ranging from 160 m to 1,640 m, and the corresponding hillslope areas range from 0.05 km^2 to 1 km^2. A lookup table enables the association between the 3-km HRRR grid and the river network. For links spanning the reach of more than one pixel, temperature estimation values are assigned as the weighted averages of the covered grid cell values. The stream temperature estimation results for 4 pm on March 30th, 2017 appear in Figure 4.9. The abnormal spatial patterns introduced by air temperature and regression parameter values disappear on the network level. For visualization purposes, only streams of 4th order and up are shown, which include 3,812 channel links.

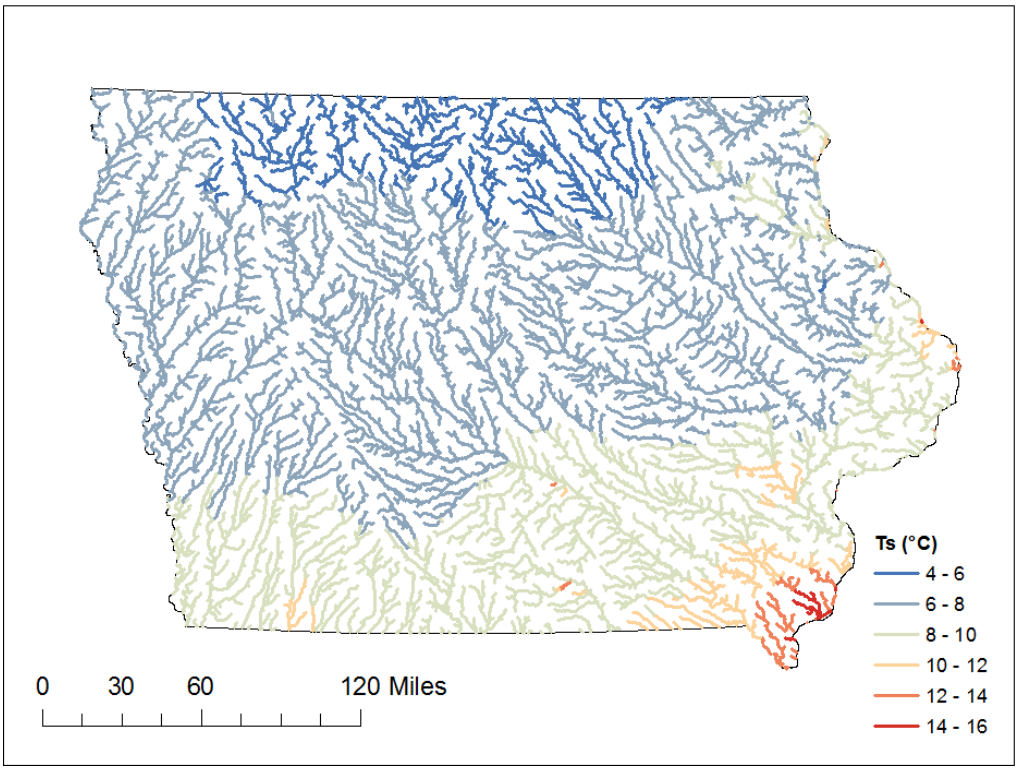

Figure 4.9 State-wide stream temperature estimations on the river network at 4 pm of March 30th, 2017.

4.6 Real-Time Visualization

State-wide estimations on the river network appear on a web-based platform: the Beta version of the Iowa Water Quality Information System, Beta version (IWQIS Beta). In accordance with the input data availability, current as well as forecasted estimations of stream temperature are available. The HRRR product updates the current and 18 hours of forecasted air temperature estimations every hour. The implemented model retrieves the newest HRRR estimations in real-time. Hence in every hour, current state-wide stream temperature estimation is available as well as forecasts for lead time of up to 18 hours. The forecasts can have hourly resolution. Certain time lag of less than 2 hours exists in HRRR data acquisition. Hence the visualized product, in fact, can present 16 hours of forecasts. The forecast interface can later be developed by IIHR as desired.

The lag time between stream and air temperatures offers a prediction advantage as we are able to associate stream temperature with the air temperature from a set number of hours ago. The number of hours is determined by the shift value at each grid cell. With 18 hours of air temperature predictions, the stream temperature model is able to provide predictions for shift number of hours on top of 18. For example, a site with 4 hours of shift time between the two temperatures would have 22 hours of predictions available. However, due to the varying numbers of shift available at each grid cell, the visualization interface would only display up to 18 hours of predictions for the entire state regardless of the actual available hours on each link. Figure 4.10 shows the IWQIS Beta real-time interface with color-coded channel links according to temperature estimations.

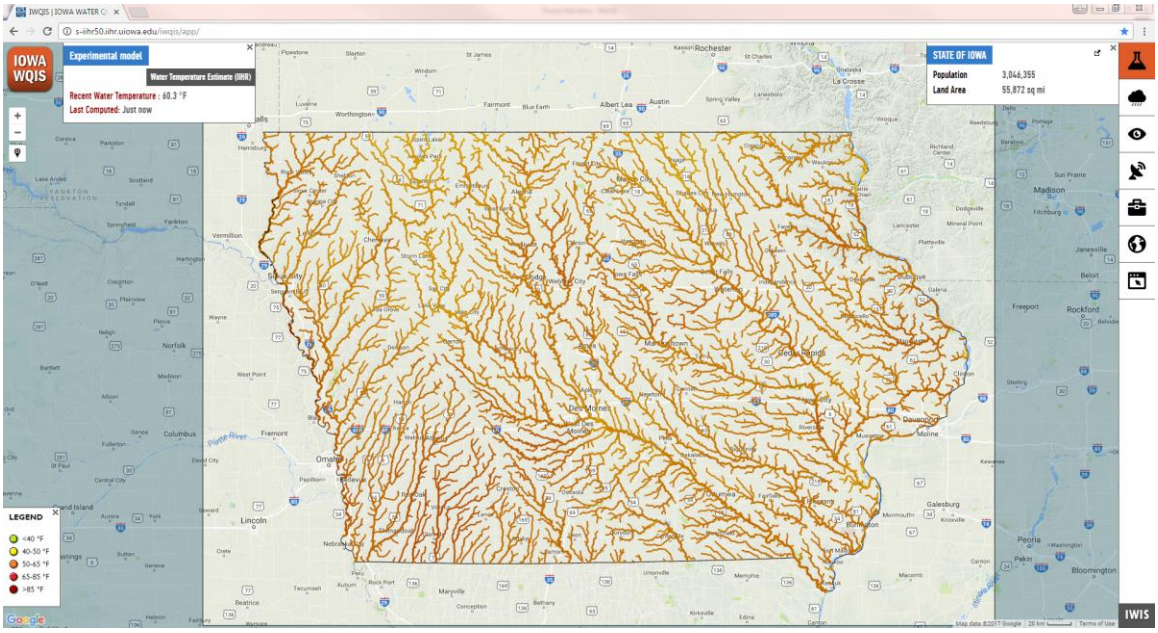

Figure 4.10 IWQIS Beta real-time state-wide stream temperature estimation interface for 4 pm of April 17th, 2017.

4.7 Chapter Summary

The logistic regression parameters estimated using historical temperature measurement data at station for each season and year were utilized to develop seasonal

site-specific models. Regression parameters α and μ were set to be the historical high and low values recorded at each site over the years for the specified seasons. Parameters β, γ, and shift were set to be the averages of the estimated values. The averages of the estimated values were parameters β, γ, and shift.

The model generated on-site stream temperature estimates for the year of 2016 using air temperature measurement data and parameter value estimates from 2012 to 2015. Model estimation results were within 3 °C average RMSE for the three seasons, with less than 1 °C standard deviation. Summer season performs the best, generating an average RMSE of less than 2 °C, with a standard deviation of less than 0.5 °C.

Site-specific parameter values were interpolated onto the cropped HRRR 3-km grid for Iowa using the inverse distance weighting method. Seasonal parameter rasters were generated for the Iowa domain, and used for gridded stream temperature estimations. Hourly updated HRRR air temperature estimations enable the hourly updates of stream temperature estimations for 19 hours, including current and forecasted conditions. The HRRR product estimates warmer air temperatures over large water bodies, leading to high stream temperature estimation results at such locations.

The state-wide gridded computational results are projected onto the hillslope-link network derived from a 90 m USGS DEM. Stream temperature estimations on the river network are updated and visualized in real-time on the IWQIS Beta web-based platform. Channel links of 4^{th} order and up are color-coded according to the estimated temperatures. The exact value of estimation can be shown when the channel link is clicked.

CHAPTER 5 CONCLUSIONS & FUTURE IMPROVEMENTS

This thesis presents the development, evaluation, and implementation of a state-wide stream temperature estimation model. The statistical model is based on the relationship between stream and air temperatures, which can be captured by a logistic function. The statistical model was initially developed at USGS and IIHR stream temperature measurement sites and later integrated onto a 3-kilometer grid that covers the entire state of Iowa. Model parameters were estimated separately for March to May (spring), June to August (summer), and September to November (autumn).

The NOAA NCEP HRRR product provides hourly air temperature inputs, which enables real-time hourly stream temperature estimations. With the grid to link association, the estimated results are transferred onto 419,157 river links throughout the state. The IWQIS Beta interface presents real-time hourly forecasts of stream temperature on the state-wide river network for a lead time of up to 18 hours and displays streams of 4^{th} order and up.

5.1 Site-Specific Model Development

Forty-five USGS and IIHR sites provide hourly stream temperature measurements in the state of Iowa. Each site has from 1 to 5 years of recorded data. The site-specific statistical models use the stream temperature measurements at the 45 locations and the air temperature measurements from most adjacent NOAA stations. Due to the seasonality in the two temperatures, the site-specific models were developed separately for spring, summer, and autumn.

The statistical model is based on the relationship between stream and air temperatures, which can be captured by a logistic function with four parameters. Due to the thermal capacity difference between water and air, stream temperature oscillations follow the air temperature oscillations with a certain time lag. Therefore, an extra model parameter is added to shift the two temperature records more in-phase with each other, hence improving the model performance. The extra parameter is named shift.

Of the four logistic regression parameters, two were found as the maximum and minimum stream temperatures within the dataset. The other two were found using least squares error method through a systematic search on a regular grid. The shift parameter was found using least squares error method through a search from 0 to 8 hours. Reservoirs and lakes were not treated as special entities in the model as the performance of model at locations downstream from reservoirs does not exhibit abnormal behavior.

5.2 Site-Specific Model Evaluation

Sensitivity analyses indicate that the model estimation performance has no direct relationship with drainage area, normalized discharge, or distance between temperature stations. However, an explanatory relationship exists between the shift parameter and drainage area size. The logistic regression model does not perform well at capturing the upper and lower tails of stream temperature, especially under freezing/thawing conditions. However, with every 5 °C change in air temperature, the first and third quartiles of hourly model estimation errors in summer stream temperatures do not exceed ±2 °C. Negligible model bias was detected.

Spatial heterogeneity exists in model performance. Western Iowa sites generally perform worse than those in the north-eastern region. Several factors could contribute to the inconsistency in performance, including different streambed formations and riparian coverage. The model performs less well in spring and autumn seasons than in summer, as the streambed and groundwater heat fluxes become more significant compared to the air-water exchange in spring and autumn. The summer season has, on average, 1.85 °C of model estimation RMSE for stream temperature, with 62.9% below the 2 °C standard for good model performance, and 89.9% below 2.5 °C. The model also performs better under normal hydrologic regimes than under dry or wet regimes.

5.3 State-Wide Model Development & Evaluation

The set seasonal site-specific model parameter values were used to estimate stream temperature in spring, summer, and autumn of 2016, which yielded results of within 3 °C average RMSE with less than 1 °C of standard deviation. Summer season average RMSE was below 2 °C, with standard deviation of less than 0.5 °C. The model parameters were interpolated onto a 3-kilometer grid throughout the state to match with the High-Resolution Rapid Refresh air temperature input resolution. Inverse distance weighting method was utilized for interpolation. Spatial heterogeneity in stream temperature estimation comes from both the explanatory variable input, and the model parameters. It appears that the NOAA NCEP HRRR product estimation of air temperature tends to be higher over large river bodies, such as reservoirs, lakes, and large rivers. The parameter raster fields vary more rapidly in space for the well-sampled eastern Iowa.

5.4 Real-Time Implementation & Visualization

The NOAA NCEP HRRR product generates real-time current and forecasted air temperature estimations, which allows for hourly updated real-time stream temperature predictions. The estimated stream temperatures on the 3-km grid are transferred onto the river network in the state through grid to link association. Estimations for streams of 4^{th} order and up appear on the IWQIS Beta platform. As HRRR provides air temperature forecasts of 18 hours in advance, state-wide stream temperature forecasts are available for lead time of up to 18 hours.

5.4 Future Improvements

The current model utilizes site-specific model parameter values for each season to estimate stream temperature. It was also previously observed that two of the logistic parameter values introduce constraints that may negatively affect the model performance. Hence one can possibly enhance the performance by setting the α and μ values (maximum and minimum stream temperature thresholds) as moving boundaries for a shorter time window than distinct seasons. An example of the annual weekly stream temperature thresholds at the Turkey River site is illustrated in Figure 5.1. One can conduct model validation using the enveloping curves for α and μ to seek enhanced performance.

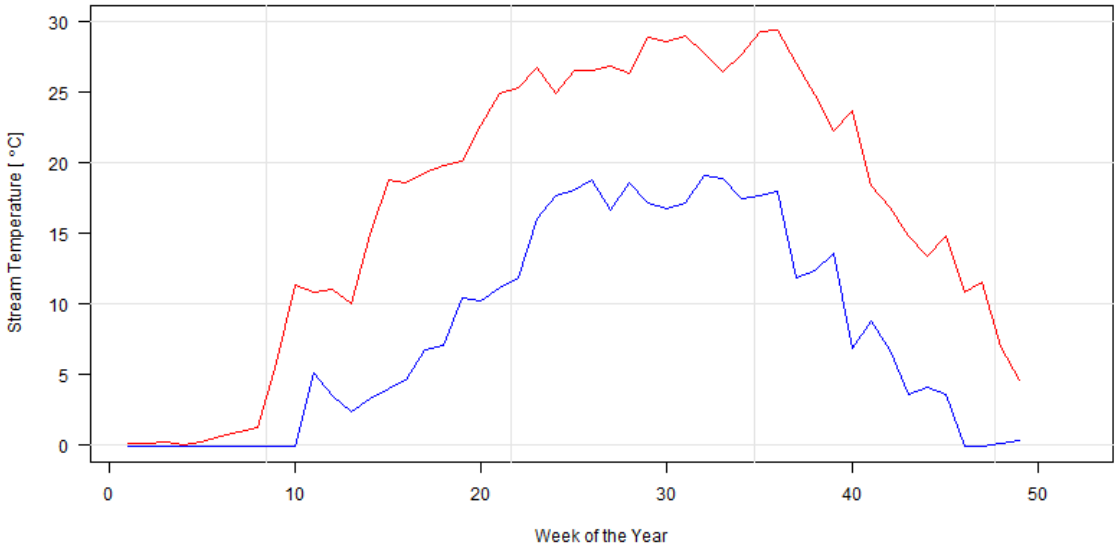

Figure 5.1 Annual weekly moving boundaries for stream temperature at the Turkey River site. Red: historical maximum weekly stream temperature. Blue: historical minimum weekly stream temperature.

The data used in the project dates back to as early as 2012 as it was readily available on the web based platforms. However, USGS most likely stores hourly stream temperature measurements for a much longer period. One could make a special request to acquire a longer record and apply the same model fitting and parameter setting procedures conducted in this project. Having a longer data record period could help us better observe the parameter distributions and model performance behavior.

In previous model evaluation analyses, it was observed that this simple regression approach does not capture the stream temperature behavior under wet or dry hydrologic regimes. The changes in air-water relation due to regime alterations can lead to poor model estimation. One can develop a simple autoregressive error model to study the residuals in the regression estimations and possibly make up for this shortcoming of the current approach.

One could also conduct Fourier analysis on stream temperature and discharge data, as not only does the temperature follow seasonal and diurnal cycles, the propagation of flow also has its own cycle. The two signals can be imposed upon or destroy each other depending on whether they are in or out of phase. This approach is similar to many stochastic models, which use Fourier series to represent the long-term stream temperature component.

As the model relies on air temperature as the explanatory variable, the quality of air temperature input is crucial to the stream temperature prediction accuracy. This thesis utilizes the meteorology model output from HRRR as it provides high resolution air temperature for the entire United States with hourly updates. However, air temperature data with higher accuracy could further enhance the stream temperature estimation performance. Meanwhile, with real-time stream temperature measurements available, data assimilation can be conducted as well to improve performance.

The travel time of water in streams can vary depending on the watershed hydrology. However, this simple statistical approach does not take basin characteristics into account. Hence the travel time effect on the air-water relationship is ignored. The width functions could accommodate this shortcoming as it accounts for water transport with respect to both time and distance, which is the partial differential component that our model lacks comparing to a deterministic model.

Statistical models for stream temperature focus mainly on the water-air temperature relationship. However, a number of physical parameters that influence stream temperature were not accounted for, including the aforementioned riparian coverage and streambed material. Additionally, shortwave radiation, watershed

hydrology, and anthropogenic perturbations were not considered by the model either. For future improvements, more variables can be studied to explain residual patterns in model performance.

The IWQIS Beta platform can also be configured to incorporate a self-evaluation mechanism that illustrates the model performance to the general public. Simple statistics of the evaluation can provide insight on the adequacy of estimation. Similarly, a time control option that allows presentation of the estimated results in the past can also be added to the platform.

5.5 Final Remarks

This thesis develops a statistical stream temperature model that uses air temperature as the only explanatory variable. There are obvious limitations to this approach. Thus the model developed and implemented in this thesis is by no means the only and best available stream temperature model. However, it is easily applicable for a large domain and requires minimal input of meteorological data. The model is also unique as it provides real-time hourly-updated estimations for the entire state, which is visualized on a web-based platform. The model performs especially well for the summer season and the product will assist Iowa water quality research and provide information to support public management decisions.

APPENDIX

Table A-1 NOAA air temperature measurement stations in Iowa (NOAA, 2017a).

NOAA Station ID	Latitude	Longitude	Elevation	Network
AMW	41.99	-93.62	280	ASOS
BRL	40.77	-91.13	213	ASOS
CID	41.88	-91.72	265	ASOS
DSM	41.53	-93.65	294	ASOS
DBQ	42.40	-90.71	329	ASOS
EST	43.40	-94.75	401	ASOS
IOW	41.64	-91.54	204	ASOS
LWD	40.63	-93.90	333	ASOS
MIW	42.11	-92.92	297	ASOS
MCW	43.15	-93.33	370	ASOS
OTM	41.10	-92.44	258	ASOS
DVN	41.61	-90.59	229	ASOS
SUX	42.39	-96.38	336	ASOS
SPW	43.17	-95.21	403	ASOS
ALO	42.55	-92.40	268	ASOS
AXA	43.08	-94.27	369	AWOS
IKV	41.69	-93.57	271	AWOS
AIO	41.41	-95.05	352	AWOS
ADU	41.70	-94.92	399	AWOS
BNW	42.05	-93.85	349	AWOS
CIN	42.04	-94.79	365	AWOS
TVK	40.68	-92.90	313	AWOS
CNC	41.02	-93.36	319	AWOS
CCY	43.07	-92.61	340	AWOS
CKP	42.73	-95.55	374	AWOS
ICL	40.72	-95.02	298	AWOS
CAV	42.74	-93.76	350	AWOS
CWI	41.83	-90.33	216	AWOS
CBF	41.26	-95.76	378	AWOS
CSQ	41.02	-94.36	393	AWOS
DEH	43.28	-91.74	353	AWOS
DNS	41.98	-95.38	381	AWOS
FFL	41.05	-91.98	242	AWOS
FXY	43.23	-93.62	375	AWOS
FOD	42.55	-94.20	355	AWOS
FSW	40.66	-91.33	220	AWOS
GGI	41.71	-92.73	307	AWOS

Table A-1 NOAA air temperature measurement stations in Iowa (NOAA, 2017a) – Continued.

HNR	41.58	-95.34	365	AWOS
IIB	42.45	-91.95	294	AWOS
IFA	42.47	-93.27	347	AWOS
EOK	40.46	-91.43	205	AWOS
OXV	41.30	-93.11	282	AWOS
LRJ	42.78	-96.19	362	AWOS
MXO	42.22	-91.16	255	AWOS
MPZ	40.95	-91.51	222	AWOS
MUT	41.37	-91.14	165.5	AWOS
TNU	41.67	-93.02	287	AWOS
OLZ	42.68	-91.98	328	AWOS
ORC	42.99	-96.06	430	AWOS
I75	41.05	-93.69	338.3	AWOS
OOA	41.23	-92.49	256	AWOS
PEA	41.40	-92.94	265	AWOS
PRO	41.83	-94.16	309	AWOS
RDK	41.01	-95.26	317	AWOS
SHL	43.21	-95.84	432	AWOS
SDA	40.75	-95.41	296	AWOS
SLB	42.60	-95.24	450	AWOS
VTI	42.22	-92.02	255	AWOS
AWG	41.28	-91.67	229	AWOS
EBS	42.44	-93.87	337	AWOS

Table A-2 Spring site-specific model evaluation results for all stations and years.

USGS Site ID	Year	alpha	miu	gamma	beta	Shift (h)	RMSE (°C)	Normalized discharge ($m^3/s\text{-}km^2$)
0546494205	2016	21.1	1.8	0.123	14.02	2	1.47	-99
06604000	2012	17.8	9.9	0.109	18.74	2	1.55	-99
06604000	2013	17.6	-0.1	0.138	9.44	1	3.36	-99
06604000	2014	22.2	3.8	0.093	15.46	2	2.73	-99
06604000	2015	17.6	2	0.116	8.79	2	3.23	-99
06604000	2016	20.9	1.5	0.1	16.91	3	3.19	-99
05418110	2013	23.1	0	0.123	13.54	3	1.91	0.0224
05418110	2014	24	0	0.121	13.19	3	2.18	0.0139
06604200	2012	19.9	0	0.097	10.1	3	3.92	-99
06604200	2013	16.8	0.1	0.124	10.73	1	2.44	-99
06604200	2014	23.7	0.4	0.096	17.38	1	3.14	-99

Table A-2 Spring site-specific model evaluation results for all stations and years – Continued.

06604200	2015	18	1.2	0.105	10.92	2	3.17	-99
06604200	2016	19.8	2.2	0.102	18.04	1	2.84	-99
05455100	2012	21.3	0.7	0.106	8.76	4	2.33	0.0096
05455100	2013	22.6	0.5	0.137	11.48	4	2.65	0.0301
05455100	2014	27.3	0	0.125	14.05	4	3.19	0.0056
05455100	2015	20.7	7.7	0.137	13.35	3	1.59	0.0094
05418400	2013	24.5	0	0.119	10.92	4	2.26	0.0213
05418400	2014	26.8	-0.1	0.124	11.77	3	2.92	0.0113
05482300	2012	26.2	7.9	0.094	17.13	4	2.22	0.0022
05482300	2013	19.7	0.3	0.148	10.26	8	2.52	0.0142
05482300	2014	26.5	0.3	0.103	11.39	3	2.81	0.0012
05482300	2015	16.6	0.5	0.109	6.98	8	3.15	0.0113
05482300	2016	20.4	1	0.104	11.36	6	2.14	0.0225
06817000	2013	25.8	-0.1	0.122	10.51	4	2.50	0.0112
06817000	2014	29.5	-0.1	0.113	14.72	4	3.54	0.0047
06817000	2015	22.4	-0.1	0.12	9.25	3	3.27	0.0122
06817000	2016	23.4	1	0.099	10.17	3	2.43	0.0160
05481000	2012	27.1	-0.1	0.1	12.11	3	3.13	0.0031
05481000	2013	20.1	-0.1	0.156	11.24	4	2.44	0.0223
05481000	2014	24.4	-0.1	0.139	13.46	4	3.44	0.0050
05481000	2015	18.9	-0.1	0.116	9.54	4	3.24	0.0118
05481000	2016	19.2	0	0.112	9.21	4	2.46	0.0162
05484000	2016	22.9	0.9	0.098	10.11	4	2.49	0.0174
06808500	2016	19.7	2.9	0.108	10.25	4	2.16	0.0175
05412500	2014	25.3	4	0.109	17.04	4	2.75	0.0216
05412500	2015	21.5	2.4	0.129	9.87	4	2.54	0.0087
05412500	2016	24.9	1.8	0.112	12.62	4	2.90	0.0141
05458300	2012	24.4	-0.1	0.1	9.6	6	3.53	0.0070
05458300	2013	19.7	0	0.156	10.96	5	2.77	0.0351
05458300	2014	23.7	-0.1	0.131	14.1	4	3.60	0.0194
05458300	2015	21.6	-0.1	0.12	10.02	5	4.05	0.0100
05458300	2016	23	0.5	0.086	14.32	5	2.81	0.0163
05482500	2012	27.3	8.7	0.108	18.53	4	2.02	0.0020
05482500	2013	23.6	0	0.142	11.58	4	2.93	0.0095
05482500	2014	27.3	-0.1	0.123	13.17	3	3.57	0.0013
05482500	2015	20.3	-0.1	0.117	8.87	4	3.64	0.0101
05482500	2016	21.7	1.5	0.102	12.93	4	2.60	0.0213

Table A-2 Spring site-specific model evaluation results for all stations and years – Continued.

05418720	2015	23.2	4.1	0.129	9.97	3	2.63	0.0076
05418720	2016	25.3	4.6	0.125	14.29	3	2.69	0.0091
05484500	2012	28.4	9.9	0.12	19.98	3	2.09	0.0038
05484500	2013	24.1	-0.1	0.136	12.04	4	2.93	0.0117
05484500	2014	27.7	-0.1	0.121	14.25	4	3.59	0.0021
05484500	2015	20.3	-0.1	0.13	8.88	4	3.37	0.0107
05484500	2016	22.7	2.2	0.102	13.35	4	2.67	0.0176
05482000	2014	22.2	0.4	0.109	13.51	6	3.55	0.0034
05482000	2015	20.8	1.5	0.113	10.68	4	3.90	0.0083
05482000	2016	23.2	2.9	0.08	15.04	3	3.54	0.0164
05464420	2013	22.2	0.1	0.14	11.04	5	3.30	0.0261
05464420	2014	25.7	0.2	0.101	13.94	4	3.60	0.0153
05464420	2015	22.4	4.5	0.127	10.5	4	2.83	0.0099
05464420	2016	24.4	1.6	0.076	15.65	5	2.96	0.0144
05487520	2012	25.5	0.9	0.096	9.9	6	3.41	0.0044
05487520	2013	22.1	-0.1	0.136	10.95	7	3.17	0.0094
05487520	2014	25.2	-0.1	0.118	13.38	6	3.91	0.0040
05487520	2015	19.7	0	0.125	7.59	6	3.72	0.0090
05487520	2016	22.6	2.3	0.098	12.49	6	3.26	0.0157
05465500	2012	26.7	11.5	0.105	20.3	5	2.60	0.0071
05465500	2013	22.2	0.1	0.119	10	7	3.44	0.0238
05465500	2014	23.2	0.1	0.117	12.84	6	3.78	0.0125
05465500	2015	23.5	0.2	0.12	10.39	5	4.35	0.0089
05465500	2016	25.3	2.4	0.106	14.03	5	3.51	0.0138

Table A-3 Summer site-specific model evaluation results for all stations and years.

USGS Site ID	Year	alpha	miu	gamma	beta	Shift (h)	RMSE (°C)	Normalized discharge ($m^3/s\text{-}km^2$)
06604000	2012	32.4	20.1	0.085	27.26	2	2.10	-99
06604000	2013	29.8	15.3	0.08	20.33	2	2.28	-99
06604000	2014	27.9	17.5	0.064	20.75	3	1.59	-99
06604000	2015	27.2	15.6	0.092	14.41	3	2.04	-99
05418110	2013	27.4	13	0.137	22.44	3	1.44	0.0134
05418110	2014	25.2	13.7	0.155	20.93	3	0.96	0.0096
06604200	2012	30	16	0.074	19.11	3	2.27	-99
06604200	2013	28.4	14.1	0.084	17.08	4	2.62	-99

Table A-3 Summer site-specific model evaluation results for all stations and years – Continued.

06604200	2014	26.6	17.5	0.076	17.11	3	1.78	-99
06604200	2015	27.6	15.7	0.084	14.9	5	2.38	-99
05455100	2012	36.3	13.7	0.127	24.6	2	1.53	0.0011
05455100	2013	31.5	14	0.13	22.79	3	2.19	0.0067
05455100	2014	28	16.8	0.123	23.46	3	1.50	0.0228
05455100	2015	28.8	14.8	0.135	22.79	3	1.86	0.0111
05418400	2014	27.8	16.8	0.151	21.76	3	1.30	0.0165
05482300	2012	34.4	13.9	0.111	21.47	4	2.31	0.0025
05482300	2013	31.6	14	0.116	23.08	4	3.26	0.0093
05482300	2014	26.4	17.1	0.104	21.19	7	1.45	0.0141
05482300	2015	27.4	13.9	0.103	20.26	7	2.99	0.0115
05482300	2016	29.8	15.4	0.097	18.08	5	2.32	0.0054
06817000	2013	33.9	14.3	0.121	20.92	4	2.55	0.0088
06817000	2014	32.1	16.6	0.09	22.97	4	2.06	0.0327
06817000	2015	31	16.7	0.128	23.9	4	1.99	0.0223
06817000	2016	32.8	18.6	0.136	24.23	4	1.89	0.0099
05481000	2012	34.9	13.8	0.119	21.2	3	2.02	0.0006
05481000	2013	32.6	14.3	0.117	24.57	4	2.66	0.0101
05481000	2014	29.7	16.4	0.102	24.9	4	1.93	0.0153
05481000	2015	30.7	14	0.124	22.92	4	2.85	0.0099
05481000	2016	29.8	15.1	0.085	25.44	4	2.38	0.0089
05484000	2016	31.3	19.6	0.131	21.81	4	1.66	0.0087
06808500	2016	29.2	17.2	0.108	24.82	4	1.62	0.0134
05412500	2013	29.3	16.8	0.139	22.04	4	1.33	0.0201
05412500	2014	27.2	16.7	0.115	21.28	4	1.62	0.0180
05412500	2015	29	16.1	0.129	22.03	4	1.69	0.0079
05412500	2016	27.1	18.8	0.126	23.21	4	1.36	0.0220
05458300	2012	31	15.7	0.077	17.95	6	2.14	0.0027
05458300	2013	28.9	13.8	0.102	21.41	4	2.44	0.0204
05458300	2014	27.7	16.7	0.087	24.3	4	1.51	0.0163
05458300	2015	28.1	17.3	0.117	22.26	5	1.62	0.0132
05482500	2012	33.4	15.4	0.105	20.25	4	2.07	0.0016
05482500	2013	31.4	15.8	0.117	22.31	4	2.78	0.0101
05482500	2014	28.7	17.8	0.109	21.42	4	1.62	0.0101
05482500	2015	30	15.8	0.121	21.8	4	2.75	0.0145
05482500	2016	30.2	18.8	0.12	21.88	4	1.86	0.0057
05418720	2015	29.6	17.6	0.13	22.78	3	1.81	0.0134

Table A-3 Summer site-specific model evaluation results for all stations and years – Continued.

05418720	2016	28	20.6	0.13	22.3	4	1.00	0.0123
05484500	2012	34.5	14.9	0.126	22.19	3	1.57	0.0014
05484500	2013	31.3	16.6	0.145	23.68	4	2.27	0.0132
05484500	2014	29.5	18.3	0.13	24.11	4	1.49	0.0120
05484500	2015	29.8	16.8	0.147	23.73	4	2.13	0.0197
05484500	2016	30.9	19.8	0.161	23.22	3	1.58	0.0061
05482000	2014	27.9	19.7	0.061	22.16	4	1.25	0.0165
05482000	2015	29.4	18.7	0.118	21.44	4	2.15	0.0115
05464420	2013	31	16.7	0.104	22.35	4	2.32	0.0232
05464420	2014	28	18.9	0.103	22.82	4	1.51	0.0197
05464420	2015	30	18.8	0.126	22.44	4	1.88	0.0125
05487520	2012	32.3	18.7	0.095	21.48	4	2.17	0.0030
05487520	2014	27.5	20.5	0.077	24.91	5	1.12	0.0154
05487520	2015	27.8	18.1	0.088	21.58	8	1.93	0.0192
05487520	2016	29.4	21.4	0.097	21.82	5	1.61	0.0089
05465500	2012	35.8	17.6	0.097	23.98	4	2.32	0.0023
05465500	2013	28.3	18.4	0.099	22.83	5	2.06	0.0192
05465500	2014	29.9	20.8	0.079	27.34	5	1.40	0.0188
05465500	2015	29	20.2	0.122	23.26	5	1.77	0.0149
05465500	2016	29.4	22.4	0.103	22.68	5	1.16	0.0145

Table A-4 Autumn site-specific model evaluation results for all stations and years.

USGS Site ID	Year	alpha	miu	gamma	beta	Shift (h)	RMSE (°C)	Normalized discharge ($m^3/s\text{-}km^2$)
06604000	2012	27.3	0.4	0.097	13.66	2	4.14	-99
06604000	2013	26.8	-0.1	0.123	11.28	1	3.91	-99
06604000	2014	24	0.3	0.119	8.1	3	3.71	-99
06604000	2015	23.9	0.4	0.114	7.54	2	3.67	-99
05418110	2013	24.6	0	0.117	11.61	3	2.36	0.0036
05418110	2014	23.7	1.7	0.106	11.98	3	2.09	0.0040
06604200	2012	25.4	1.8	0.09	12.3	2	3.77	-99
06604200	2013	27.2	1.6	0.124	10.92	3	3.76	-99
06604200	2014	24.2	0.5	0.115	6.81	3	3.52	-99
06604200	2015	25.6	2.3	0.092	8.86	4	3.20	-99
05455100	2012	31	0	0.106	16.07	2	2.97	0.0005
05455100	2013	28.5	0	0.15	13.85	4	2.82	0.0003
05455100	2014	24.7	0.7	0.104	10.77	4	2.78	0.0103

Table A-4 Autumn site-specific model evaluation results for all stations and years – Continued.

05455100	2015	28.4	6.5	0.128	18.17	3	2.49	0.0082
05418400	2013	27.4	0	0.132	12.16	3	2.62	0.0045
05418400	2014	25.9	2.9	0.132	13.04	3	2.61	0.0055
05482300	2012	27.1	2.2	0.108	14.63	4	2.97	0.0002
05482300	2013	28.8	-0.1	0.132	13.03	3	2.97	0.0003
05482300	2014	22.3	0	0.137	8.74	8	3.24	0.0067
05482300	2015	24.9	4.8	0.121	13.98	6	2.55	0.0127
05482300	2016	25.9	1.7	0.11	12.13	5	3.05	0.0151
06817000	2013	31.6	-0.1	0.155	14.84	5	3.57	0.0009
06817000	2014	25.2	-0.1	0.119	11.41	5	3.76	0.0222
06817000	2015	30	1.3	0.103	15.1	4	3.25	0.0122
06817000	2016	29	2	0.102	14.73	4	3.20	0.0088
05481000	2012	30.4	0.9	0.103	17.21	4	3.26	0.0002
05481000	2013	29.2	-0.1	0.141	13.54	4	3.20	0.0002
05481000	2014	22.7	-0.1	0.133	9.66	5	3.36	0.0075
05481000	2015	25.4	-0.1	0.11	11.67	4	3.07	0.0052
05481000	2016	26	0.9	0.098	13.3	5	3.35	0.0243
05484000	2016	29	2.5	0.1	14.39	3	3.42	0.0083
06808500	2016	25.6	3.6	0.107	14.9	4	2.98	0.0131
05412500	2013	27.4	-0.1	0.116	12.75	4	3.31	0.0032
05412500	2014	25.4	2	0.109	11.9	4	3.05	0.0042
05412500	2015	29.4	-0.1	0.11	14.31	3	3.21	0.0031
05412500	2016	23.4	2.8	0.112	13.13	5	2.86	0.0256
05458300	2012	25	0.4	0.101	11.91	8	3.68	0.0014
05458300	2013	26.5	-0.1	0.128	11.62	7	3.58	0.0034
05458300	2014	25	-0.1	0.124	11.14	5	3.67	0.0052
05458300	2015	27.3	0.8	0.112	13.43	6	3.60	0.0058
05482500	2012	29.2	0	0.098	15.13	4	3.69	0.0002
05482500	2013	28.6	0	0.132	12.63	4	3.65	0.0003
05482500	2014	23.4	-0.1	0.132	9.51	4	3.63	0.0106
05482500	2015	25	4.5	0.104	14.1	6	3.60	0.0147
05482500	2016	27.7	1.8	0.101	14.32	4	3.59	0.0112
05418720	2015	29.2	1.1	0.115	14.14	3	3.41	0.0071
05418720	2016	26.2	3.2	0.118	14.02	4	3.37	0.0099
05484500	2012	31.2	-0.1	0.107	16.44	3	2.95	0.0004
05484500	2013	29	-0.1	0.135	14.06	4	3.13	0.0006
05484500	2014	23.8	-0.1	0.134	10.96	5	3.32	0.0161
05484500	2015	27	3.5	0.123	15.7	4	3.02	0.0132
05484500	2016	28.6	2.8	0.105	15.66	4	3.11	0.0089

Table A-4 Autumn site-specific model evaluation results for all stations and years – Continued.

05482000	2014	26	0.8	0.118	10.67	5	3.83	0.0061
05482000	2015	26.5	5.1	0.119	13.17	5	3.36	0.0075
05482000	2016	26.9	6.6	0.103	14.24	3	3.41	0.0137
05464420	2013	28.8	1.3	0.119	12.76	4	3.67	0.0028
05464420	2014	25.6	1.8	0.12	10.89	4	3.62	0.0052
05464420	2015	28.7	1.8	0.121	13.16	4	3.73	0.0069
05487520	2012	29.8	1.4	0.093	13.85	3	4.04	0.0004
05487520	2013	29.7	0.3	0.117	12.65	4	4.03	0.0008
05487520	2014	24.2	-0.1	0.125	9.64	7	3.77	0.0130
05487520	2015	25.7	3.7	0.124	13.72	6	3.56	0.0095
05487520	2016	26.6	5.3	0.116	15.07	5	3.71	0.0105
05465500	2012	20.4	-0.1	0.112	8.79	5	3.28	0.0010
05465500	2013	28.6	0.1	0.104	14.54	7	3.47	0.0019
05465500	2014	27	-0.1	0.111	11.97	5	4.08	0.0067
05465500	2015	28.1	3.2	0.119	13.76	5	3.78	0.0080

Table A-5 Spring site-specific parameters for model implementation.

Water Temperature Site ID	Number of years	alpha	beta	miu	gamma	shift (h)
06604000	4	22.2	13.11	-0.100	0.1140	2
05418110	2	24.0	13.37	0.000	0.1220	3
06604200	4	23.7	12.28	0.000	0.1055	2
05455100	4	27.3	11.91	0.000	0.1263	4
05418400	2	26.8	11.35	-0.100	0.1215	4
05482300	4	26.5	11.44	0.300	0.1135	6
06817000	3	29.5	11.49	-0.100	0.1183	4
05481000	4	27.1	11.59	-0.100	0.1278	4
05412500	2	25.3	13.46	2.400	0.1190	4
05458300	4	24.4	11.17	-0.100	0.1268	5
05482500	4	27.3	13.04	-0.100	0.1225	4
05418720	1	23.2	9.97	4.100	0.1290	3
05484500	4	28.4	13.79	-0.100	0.1268	4
05482000	2	22.2	12.10	0.400	0.1110	5
05464420	3	25.7	11.83	0.100	0.1227	4
05487520	4	25.5	10.46	-0.100	0.1188	6
05465500	4	26.7	13.38	0.100	0.1153	6
1	2	24.8	11.01	0.000	0.0925	4
2	1	21.5	12.17	3.30	0.1310	3

Table A-5 Spring site-specific parameters for model implementation – Continued.

3	2	24.9	11.89	-0.06	0.1135	3
5	2	24.3	13.90	5.47	0.1175	6
6	1	22.8	11.57	5.60	0.1120	4
9	1	19.5	11.05	5.32	0.1520	2
10	1	22.6	13.65	11.00	0.1400	4
11	1	19.5	11.83	0.76	0.1210	2
12	1	18.5	14.84	0.39	0.1150	1
14	1	23.1	13.27	0.01	0.1210	2
16	1	19.4	13.13	3.12	0.1460	2
17	1	21.3	12.22	4.13	0.1390	1
18	1	23.3	12.91	5.15	0.1410	2
21	1	17.2	11.22	0.83	0.1210	3
22	1	17.3	12.58	1.41	0.1180	2

Table A-6 Summer site-specific parameters for model implementation.

Water Temperature Site ID	Number of years	alpha	beta	miu	gamma	shift (h)
06604000	4	29.3	20.7	17.13	0.0803	2
05418110	2	26.3	21.7	13.35	0.1460	3
06604200	4	28.2	17.1	15.83	0.0795	4
05455100	4	31.2	23.4	14.83	0.1288	3
05418400	1	27.8	21.8	16.80	0.1510	3
05482300	4	30.0	21.5	14.73	0.1085	6
06817000	3	32.3	22.6	15.87	0.1130	4
05481000	4	32.0	23.4	14.63	0.1155	4
05412500	3	28.5	21.8	16.53	0.1277	4
05458300	4	28.9	21.5	15.88	0.0958	5
05482500	4	30.9	21.4	16.20	0.1130	4
05418720	1	29.6	22.8	17.60	0.1300	3
05484500	4	31.3	23.4	16.65	0.1370	4
05482000	2	28.7	21.8	19.20	0.0895	4
05464420	3	29.7	22.5	18.13	0.1110	4
05487520	3	29.2	22.7	19.10	0.0867	6
05465500	4	30.8	24.4	19.25	0.0993	5
1	2	27.5	21.7	21.06	0.0710	4
2	2	28.7	23.9	15.09	0.1290	3
3	2	32.7	26.6	14.15	0.1155	4
4	1	28.6	25.6	13.19	0.1210	3

Table A-6 Summer site-specific parameters for model implementation – Continued.

5	2	29.1	23.9	17.60	0.1090	5
6	1	28.1	21.0	20.21	0.1170	5
7	1	38.5	30.0	16.14	0.0730	1
8	2	29.8	22.0	15.93	0.1410	2
9	1	24.7	21.5	13.18	0.1470	2
10	1	27.8	20.8	18.70	0.1150	5
11	1	25.3	21.0	10.78	0.1290	2
12	1	20.2	18.8	9.14	0.1260	2
13	1	26.8	21.9	12.05	0.1600	3
14	1	35.0	23.1	10.71	0.2040	1
16	1	24.6	20.8	10.38	0.1330	3
17	1	28.6	21.3	11.95	0.1590	1
19	1	31.6	22.9	14.31	0.1390	3
21	1	24.1	22.4	10.14	0.1270	3
22	1	22.8	22.0	10.09	0.1340	2

Table A-7 Autumn site-specific parameters for model implementation.

Water Temperature Site ID	Number of years	alpha	beta	miu	gamma	shift (h)
06604000	4	27.3	10.145	-0.1	0.11325	2
05418110	2	24.6	11.795	0	0.1115	3
06604200	4	27.2	9.7225	0.5	0.10525	3
05455100	4	31	14.715	0	0.122	3
05418400	2	27.4	12.6	0	0.132	3
05482300	4	28.8	12.595	-0.1	0.1245	5
06817000	3	31.6	13.7833	-0.1	0.12567	5
05481000	4	30.4	13.02	-0.1	0.12175	4
05412500	3	29.4	12.9867	-0.1	0.11167	4
05458300	4	27.3	12.025	-0.1	0.11625	6
05482500	4	29.2	12.8425	-0.1	0.1165	4
05418720	1	29.2	14.14	1.1	0.115	3
05484500	4	31.2	14.29	-0.1	0.12475	4
05482000	2	26.5	11.92	0.8	0.1185	5
05464420	3	28.8	12.27	1.3	0.12	4
05487520	4	29.8	12.465	-0.1	0.11475	5
05465500	4	28.6	12.265	-0.1	0.1115	6
1	3	29.4975	11.1633	0.70333	0.1	4
2	3	30.15	14.6767	-0.1	0.12467	2

Table A-7 Autumn site-specific parameters for model implementation – Continued.

3	3	28.9825	13.93	-0.0617	0.13133	3
4	2	26.12	12.69	0.225	0.1235	4
5	3	28.2	18.62	0.225	0.08933	7
6	1	39.965	21.63	-0.1	0.082	3
7	2	29.63	12.97	-0.0425	0.105	5
8	1	29.4408	16.11	2.12333	0.11	2
9	2	23.8275	11.71	0.65417	0.1065	2
10	2	26.6058	12.125	-0.1	0.11	4
11	1	28.0208	16.93	5.11083	0.119	2
12	1	19.1317	13.78	6.13	0.137	3
13	1	26.495	15.84	3.26667	0.12	2
14	1	34.2373	18.84	2.33	0.124	2
16	1	24.8492	16.64	3.92583	0.118	3
17	1	27.925	14.68	0	0.107	2
19	1	30.7767	19.23	5.19167	0.118	3
21	1	23.18	14.96	5.64083	0.122	2
22	1	22.6708	14.53	5.09667	0.132	3

Table A-8 2016 on-site evaluation for spring, summer, and autumn using parameter value estimates from 2012 to 2015.

Water Temperature Site ID	Spring RMSE (°C)	Summer RMSE (°C)	Autumn RMSE (°C)
06604000	3.43	2.08	3.58
06604200	3.89	2.37	3.43
05482300	3.51	2.71	3.38
06817000	3.81	2.00	3.88
05481000	4.14	2.84	4.30
05412500	2.94	1.45	3.73
05458300	3.39	1.13	3.63
05482500	3.59	2.01	3.86
05418720	3.45	1.42	3.51
05484500	3.58	2.11	3.68
05482000	3.81	2.12	3.78
05464420	3.56	1.29	3.63
05487520	3.88	2.06	4.06
05465500	3.65	1.75	3.45
1	3.80	1.81	3.54
2	2.08	1.61	1.36
3	2.00	1.42	2.88

Table A-8 2016 on-site evaluation for spring, summer, and autumn using parameter value estimates from 2012 to 2015 – Continued.

8	--	2.02	2.86
9	1.65	1.14	2.25
11	1.35	1.39	1.56
12	1.82	1.54	1.82
13	--	1.20	2.23
14	1.77	2.54	2.87
16	1.40	1.13	1.76
21	1.43	1.60	1.51
22	--	1.33	1.54

REFERENCES

Beschta, R. L. (1997). Riparian shade and stream temperature: an alternative perspective. *Rangelands*, *19*(2), 25–28.

Brown, G. W. (1969). Predicting Temperatures of Small Streams. *Water Resources Research*, *5*(1), 68–75. https://doi.org/10.1029/WR005i001p00068

Caissie, D. (2006). The thermal regime of rivers: A review. *Freshwater Biology*, *51*(8), 1389–1406. https://doi.org/10.1111/j.1365-2427.2006.01597.

Caissie, D., El-Jabi, N., & St-Hilaire, a. (1998). Stochastic modelling of water temperatures in a small stream using air to water relations. *Canadian Journal of Civil Engineering*, *25*(2), 250–260. https://doi.org/10.1139/cjce-25-2-250

Caissie, D., St-Hilaire, A., & El-Jabi, N. (2004). Prediction of Water Temperatures Using Regression and Stochastic Models. *57th Canadian Water Ressources Association Annual Congress*, *57*, 1–16.

Chen, D., Carsel, R. F., McCutcheon, S. C., & Nutter, W. L. (1998). Stream Temperature Simulation of Forested Riparian Areas: I. Watershed-Scale Model Development. *Journal of Environmental Engineering-Asce*, *124*(2), 122–130. https://doi.org/10.1061/(ASCE)0733-9372(1998)124

Chen, G., & Fang, X. (2015). Accuracy of Hourly Water Temperatures in Rivers Calculated from Air Temperatures. *Water*, *7*(3), 1068–1087. https://doi.org/10.3390/w7031068

Chenard, J. F., & Caissie, D. (2008). Stream temperature modelling using artificial neural networks: application on Catamaran Brook, New Brunswick, Canada. *Hydrological Processes*, *22*(17), 3361–3372. https://doi.org/10.1002/hyp.6928

Cluis, D. A. (1972). Relationship between stream water temperature and ambient air temperature - A simple autoregressive model for mean daily stream water temperature fluctuations.

Crumpton, W. G., Stenback, G. a, Miller, B. A., & Helmers, M. J. (2006). Potential Benefits of Wetland Filters for Tile Drainage Systems : Impact on Nitrate Loads to Mississippi River Subbasins. *Agricultural and Biosystems Engineering Technical Reports and White Papers.*, (December).

EPA. (2016). Regional Monitoring Networks (RMNs) to Detect Changing Baselines in Freshwater Wadeable Streams.

Evans, E. C., McGregor, G. R., & Petts, G. E. (1998). River energy budgets with special reference to river bed processes. *Hydrological Processes*, *12*(April 1997), 575–595. https://doi.org/10.1002/(SICI)1099-1085(19980330)12:4<575::AID-HYP595>3.0.CO;2-Y

Ficklin, D. L., Luo, Y., Stewart, I. T., & Maurer, E. P. (2012). Development and application of a hydroclimatological stream temperature model within the Soil and Water Assessment Tool. *Water Resources Research*, *48*(1), 1–16. https://doi.org/10.1029/2011WR011256

Iowa Department of Natural Resources and Iowa Geological Survey. (2017). Natural Resources Geographical Information Systems Library. Retrieved from https://programs.iowadnr.gov/nrgislibx/

Iowa State University Extension and Outreach. (2017). Soil and Land Use. Retrieved from http://www.extension.iastate.edu/soils/crop-and-land-use-statewide-data

Jeppesen, E., & Iversen, T. M. (1987). Two simple models for estimating daily mean water temperatures and diel variations in a Danish low gradient stream. *Oikos*, *49*(2), 149–155. https://doi.org/10.2307/3566020

Jourdonnais, J. H., Walsh, R. P., Pickett, F. J., & Goodman, D. (1992). Structure and calibration strategy for a water temperature model of the lower Madison River, Montana.

Mohseni, O., & Stefan, H. G. (1999). Stream temperature/air temperature relationship: A physical interpretation. *Journal of Hydrology*, *218*(3–4), 128–141. https://doi.org/10.1016/S0022-1694(99)00034-7

Mohseni, O., Stefan, H. G., & Erickson, T. R. (1998). A nonlinear regression model for weekly stream temperatures. *Water Resources Research*, *34*(10), 2685. https://doi.org/10.1029/98WR01877

Nelson, K. C., & Palmer, M. A. (2007). Stream temperature surges under urbanization and climate change: Data, models, and responses. *Journal of the American Water Resources Association*, *43*(2), 440–452. https://doi.org/10.1111/j.1752-1688.2007.00034.x

NOAA. (2017a). State Climate Extremes Committee (SCEC). Retrieved from https://www.ncdc.noaa.gov/extremes/scec/records

NOAA. (2017b). The High-Resolution Rapid Refresh (HRRR). Retrieved from https://rapidrefresh.noaa.gov/hrrr/

Rutherford, J. C., Marsh, N. A., Davies, P. M., & Bunn, S. E. (2004). Effects of patchy shade on stream water temperature: How quickly do small streams heat and cool? *Marine and Freshwater Research*, *55*(8), 737–748. https://doi.org/10.1071/MF04120

Segura, C., Caldwell, P., Sun, G., Mcnulty, S., & Zhang, Y. (2015). A model to predict stream water temperature across the conterminous USA. *Hydrological Processes*, *29*(9), 2178–2195. https://doi.org/10.1002/hyp.10357

Sinokrot, B. A., & Stefan, H. G. (1993). Stream temperature dynamics: measurement and modeling. *Water Resources Research*, *29*(7), 2299–2312.

Sinokrot, B. A., & Stefan, H. G. (1994). Stream Water-Temperature Sensitivity to Weather and Bed Parameters. *Journal of Hydraulic Engineering*, *120*(6), 722–736.

Stella, J. M. (2013). Stream water temperature simulation models : a review. *Revista Sociedad Uruguaya de Geología*, *19*, 10–19.

V. Kothandaraman. (1971). Analysis of Water Temperature Variations in Large River. *ASCE Sanitary Engineering Division Journal*, *97*.

Webb, B. W., Clack, P. D., & Walling, D. E. (2003). Water-air temperature relationships in a Devon river system and the role of flow. *Hydrological Processes*, *17*(15), 3069–3084. https://doi.org/10.1002/hyp.1280

Westhoff, M. C., Savenije, H. H. G., Luxemburg, W. M. J., Stelling, G. S., van de Giesen, N. C., Selker, J. S., … Uhlenbrook, S. (2007). A distributed stream temperature model using high resolution temperature observations. *Hydrology and Earth System Sciences*, *11*, 1469–1480. https://doi.org/10.5194/hessd-4-125-2007

Younus, M., Hondzo, M., & Engel, B. A. (2000). Stream Temprature Dynamics in Upland Agricultural Watersheds, (June), 518–526.